

## Geological Society of America Bulletin

### Trace-element transport during subduction-zone ultrahigh-pressure metamorphism: Evidence from western Tianshan, China

Yuanyuan Xiao, Shaun Lavis, Yaoling Niu, Julian A. Pearce, Huaikun Li, Huichu Wang and Jon Davidson

*Geological Society of America Bulletin* 2012;124, no. 7-8;1113-1129  
doi: 10.1130/B30523.1

---

**Email alerting services**

click [www.gsapubs.org/cgi/alerts](http://www.gsapubs.org/cgi/alerts) to receive free e-mail alerts when new articles cite this article

**Subscribe**

click [www.gsapubs.org/subscriptions/](http://www.gsapubs.org/subscriptions/) to subscribe to Geological Society of America Bulletin

**Permission request**

click <http://www.geosociety.org/pubs/copyrt.htm#gsa> to contact GSA

Copyright not claimed on content prepared wholly by U.S. government employees within scope of their employment. Individual scientists are hereby granted permission, without fees or further requests to GSA, to use a single figure, a single table, and/or a brief paragraph of text in subsequent works and to make unlimited copies of items in GSA's journals for noncommercial use in classrooms to further education and science. This file may not be posted to any Web site, but authors may post the abstracts only of their articles on their own or their organization's Web site providing the posting includes a reference to the article's full citation. GSA provides this and other forums for the presentation of diverse opinions and positions by scientists worldwide, regardless of their race, citizenship, gender, religion, or political viewpoint. Opinions presented in this publication do not reflect official positions of the Society.

---

**Notes**

# Trace-element transport during subduction-zone ultrahigh-pressure metamorphism: Evidence from western Tianshan, China

Yuanyuan Xiao<sup>1,2,†</sup>, Shaun Lavis<sup>3</sup>, Yaoling Niu<sup>1,2,†</sup>, Julian A. Pearce<sup>3</sup>, Huaikun Li<sup>4</sup>, Huichu Wang<sup>4</sup>, and Jon Davidson<sup>1</sup>

<sup>1</sup>Department of Earth Sciences, Durham University, Durham DH1 3LE, UK

<sup>2</sup>School of Earth Sciences, Lanzhou University, Lanzhou 730000, China

<sup>3</sup>School of Earth and Ocean Sciences, Cardiff University, Cardiff CF10 3YE, UK

<sup>4</sup>Tianjin Institute of Geology and Mineral Resources, Tianjin 300170, China

## ABSTRACT

Subduction-zone metamorphism is considered to be a major chemical filter for both the arc magmatism and mantle compositional heterogeneity. To understand the element transport during this process, we conducted a petrographic and geochemical study of the bulk-rock blueschists and eclogites from the western Tianshan ultrahigh-pressure metamorphic belt, northwest China. By examining correlations among incompatible elements, we show that high field strength elements (HFSEs), rare earth elements (REEs), Th, and U are relatively immobile, whereas Pb and Sr are mobile in both basaltic and sedimentary protoliths during subduction-zone metamorphism. K, Rb, Cs, and Ba are mobile in rocks of basaltic protolith but immobile in rocks of sedimentary protolith because of the presence and persistent stability of white mica throughout their petrologic history. The commonly observed enrichment of some immobile elements (e.g., U, light [L] REEs) in arc magmas may thus not be caused by subduction-zone aqueous fluids.

The lack of Rb/Sr-Sm/Nd correlation in these metamorphosed rocks is inconsistent with the observed first-order Sr-Nd isotope correlation in oceanic basalts, suggesting that the residual ocean crust that has undergone subduction-zone metamorphism cannot be the major source material for oceanic basalts, as widely believed, although it can contribute to mantle compositional heterogeneity in general.

## INTRODUCTION

One of the major advances in the field of solid earth geochemistry over the past ~40 yr is the recognition of mantle chemical and isotopic heterogeneity through studies of oceanic basalts, including mid-ocean-ridge basalt (MORB) and basalts erupted on intraplate volcanic islands (or ocean island basalts [OIBs]). OIBs are particularly variable in composition, such that several isotopically distinct end members, e.g., enriched mantle I (EMI), enriched mantle II (EMII), high  $\mu$  (HIMU;  $\mu = {}^{238}\text{U}/{}^{204}\text{Pb}$ ), are required to explain the variability (e.g., White, 1985; Zindler and Hart, 1986). The depleted MORB mantle (DMM) is thought to have resulted from the extraction of continental crust from the primitive mantle early in Earth's history (e.g., O'Nions et al., 1979), but the origin of OIB end members remains enigmatic. Isotopic ratio differences among these end members reflect the differences in ratios of radioactive parent (P) over radiogenic daughter (D) elements (i.e., P/D) (e.g., Rb/Sr, Sm/Nd, U/Pb, and Th/Pb; Zindler and Hart, 1986) in their ultimate mantle sources, which evolve with time to distinctive fields in isotopic ratio spaces (see Niu and O'Hara, 2003). Significant P-D element fractionations in the solid state are considered unlikely in the deep mantle due to extremely slow diffusion rates (Hofmann and Hart, 1978); hence, processes known to occur in the upper mantle and crust (e.g., partial melting, magma evolution, metamorphism, weathering, transportation, and sedimentation) are possible causes of P-D fractionations (Niu and O'Hara, 2003). Among other processes, mantle metasomatism can effectively cause mantle compositional heterogeneity (e.g., Sun and McDonough, 1989) and may take place at the base of the growing oceanic lithosphere (e.g., Niu and O'Hara, 2003; Pilet et al., 2008)

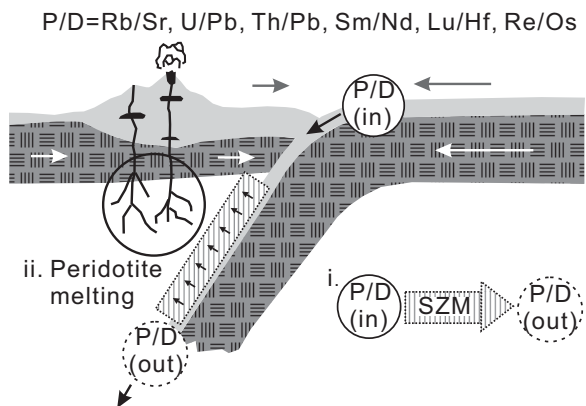
or in the mantle wedge above subduction zones (Donnelly et al., 2004).

As an inevitable consequence of plate tectonics, subduction of shallow- and surface-processed materials must volumetrically be the major agent that causes mantle compositional heterogeneity. This has led to the contention that mantle heterogeneity can be related to specific subducted components. For example, (1) altered ocean crust with high U/Pb ratio and appropriate values for other P/D ratios (e.g., Weaver, 1991; Hofmann, 1997) could produce mantle sources with HIMU characteristics; (2) land-derived sediments or upper continental crust materials (e.g., Weaver, 1991; Hofmann, 1997; Willbold and Stracke, 2006) may contribute to EMII-type lavas; and (3) pelagic sediments (e.g., Weaver, 1991) or lower continental crust (Willbold and Stracke, 2006) may contribute to EMI-type lavas.

While these interpretations are apparently reasonable, they cannot be validated without understanding the geochemical effects of subduction-zone metamorphism. This is because metamorphic dehydration of subducting ocean crust, which has been widely accepted to cause mantle wedge melting for arc magmatism (e.g., McCulloch and Gamble, 1991), may be accompanied by chemical modification resulting from elemental transport in released fluids. As illustrated in Figure 1, the subducted component (i.e.,  $[\text{P}/\text{D}]_{\text{[in]}}$ ) is modified as it passes through the "subduction factory" (e.g., Tatsumi and Kogiso, 2003) (i.e.,  $[\text{P}/\text{D}]_{\text{[out]}}$ ), so this process needs to be accounted for in any realistic mass balance models. We cannot indiscriminately treat the compositions of subducted/subducting sediments (of various types) or altered ocean crust as source materials for oceanic basalts without understanding the effects of subduction-zone metamorphism because it is the geochemical properties of  $[\text{P}/\text{D}]_{\text{[out]}}$  that contribute to mantle

<sup>†</sup>E-mails: [yuanyuan.xiao@durham.ac.uk](mailto:yuanyuan.xiao@durham.ac.uk); [yaoling.niu@durham.ac.uk](mailto:yaoling.niu@durham.ac.uk)

**Figure 1. Schematic diagram showing the likely changes of the subducted materials and the possible effects on elemental ratios of radioactive parent over radiogenic daughter isotopes (P/D) by dehydration-dominated subduction-zone metamorphism (SZM) (i), which is also widely accepted to cause the mantle wedge melting for arc magmatism (ii). Conceptually, it is the P/D ratio of the residual materials passing through subduction-zone metamorphism that determines the mantle chemical and, with time, isotopic heterogeneities recognized in oceanic basalts (after Niu, 2009).**



compositional heterogeneity with P/D and isotopic imprints.

Experimental and modeling approaches (e.g., Pawley and Holloway, 1993; Schmidt and Poli, 1998) to subduction-zone metamorphism are useful, but their applications are not straightforward because the natural system is open and complex, and there are many potential protolith types and metamorphic conditions (Zack and John, 2007; Schmidt and Poli, 2003). Thus, the analysis of natural rocks, which have actually subducted and been exhumed, remains essential in understanding the effects of subduction-zone metamorphism. However, only a few suites of subduction-related high-pressure (HP) metamorphic rocks are recognized globally, even much less for ultrahigh-pressure (UHP) metamorphic rocks, e.g., 2.7–2.9 GPa in Lago di Cignana (e.g., Reinecke, 1998) and 2.6–2.8 GPa in central Zambia (John et al., 2004). The geochemical consequences of subduction-zone metamorphism and their controls have been reported in recent studies (e.g., Spandler et al., 2004; Bebout, 2007), but the results are inconclusive and more work is needed. We chose to study subduction-zone metamorphic rocks from the western Tianshan, China, because these rocks experienced ultrahigh-pressure metamorphism as evidenced by the presence of coesite (e.g., Zhang et al., 2005; Lü et al., 2008, 2009) and other preserved UHP metamorphic reactions (Zhang et al., 2003). Therefore, the results of our study on these UHP metamorphic rocks will contribute to understanding the geochemical effects of UHP metamorphism and offer insights into processes occurring beneath the volcanic arc.

Based on mineral modal analyses and detailed correlation analyses of most analyzed elements in these rocks, we found varying element mobility/immobility during subduction-zone metamorphism, and we try to identify the pos-

sible controls on the geochemical behavior of these elements in subducting/subducted ocean crust and sediments. In addition, in terms of P/D and isotopic systematics observed in oceanic basalts, we want to test whether the representative subducted ocean crust could be a major source material for oceanic basalts.

## GEOLOGICAL BACKGROUND

### Overview of Western Tianshan Mountains

The Chinese western Tianshan orogenic belt separates the Junggar plate to the north from the Tarim plate to the south. Between the Tarim and Junggar plates, the Yili–Central Tianshan plate is defined by the north-central Tianshan suture and south-central Tianshan suture for its northern and southern boundaries, respectively (Fig. 2; Zhang et al., 2001). The UHP metamorphic belt is located along the south-central Tianshan suture, which is thought to continue to the west in Kazakhstan (e.g., Volkova and Budanov, 1999). It defines the convergent margin associated with northward subduction of the south Tianshan Devonian seafloor beneath the Yili–Central Tianshan plate, which was followed by the northward subduction of the Tarim plate upon closure of the south Tianshan ocean basin (e.g., Gao and Klemd, 2003; Fig. 2).

Much effort has been expended to date the peak metamorphic event using a variety of techniques, including the Ar–Ar plateau method (e.g., Gao and Klemd, 2003) and the Sm–Nd and Rb–Sr isochron methods (Gao and Klemd, 2003), the latter of which gave an age of ca. 350–345 Ma (Carboniferous) for peak metamorphism and ca. 311–310 Ma for exhumation (i.e., cooling age) (details are given in Gao et al., 2006). Much younger ages of  $233 \pm 4$  Ma to  $226 \pm 4.6$  Ma (Triassic) have been obtained using the sensitive high-resolution ion micro-

probe (SHRIMP) U–Pb method on metamorphic zircons extracted from both blueschist and UHP eclogite (Zhang et al., 2007). However, from the most recent zircon SHRIMP U–Pb ages reported by Gao et al. (2009) and Su et al. (2010), as well as the constraints on the cooling age of ca. 311 Ma (Lifei Zhang, 2010, personal commun.), it is apparent that the peak metamorphism happened in the Carboniferous Period (vs. Triassic) in western Tianshan.

Existing work has argued that the western Tianshan HP and UHP metamorphic rocks experienced subduction and ultimate exhumation of ocean crust in response to a continental collision event, with a clockwise pressure-temperature-time ( $P$ - $T$ - $t$ ) path on a regional scale and nearly isothermal decompression from peak eclogite facies to epidote-amphibolite facies (e.g., Gao and Klemd, 2003). The protoliths are argued to be dominated by seafloor basalts, including OIB, normal N-type, and enriched E-type MORB, as well as volcanic arc basalts (e.g., Gao and Klemd, 2003), with some terrigenous sediments (e.g., Ai et al., 2006). The highly variable compositions of metabasaltic rocks are consistent with the geochemistry of seamounts like those near the East Pacific Rise (see Niu and Batiza, 1997). Intermingled with terrigenous sediments and volcanoclastic rocks, those dismembered basalts formed a tectonic mélange within an accretionary wedge before the subsequent subduction and UHP metamorphism (e.g., Gao and Klemd, 2003; Ai et al., 2006).

### UHP Metamorphism in Western Tianshan Mountains

Despite the debate over the past ~10 yr on the peak  $P$ - $T$  conditions of western Tianshan metamorphism (e.g., Zhang et al., 2002a, 2002b; Klemd, 2003), the discovery of coesite from western Tianshan eclogites (Lü et al., 2008, 2009) gives smoking gun evidence in support of UHP metamorphism with peak pressures in excess of 2.5 GPa.

Coesite as inclusions in garnet of Tianshan eclogites has been inferred to be widespread (Lü et al., 2008, 2009; Lifei Zhang, 2010, personal commun.), and so the dispute on whether or not UHP metamorphism took place in the western Tianshan orogenic belt is settled, and any argument against UHP metamorphism by neglecting the presence of coesite is no longer valid. Nevertheless, it is worthwhile to go over briefly the history with the aim of correctly informing the international community of the nature of the dispute. Prior to the discovery of coesite, applications of geothermobarometry to Tianshan eclogite samples (including our samples) led some authors (e.g., Klemd, 2003; Lavis,

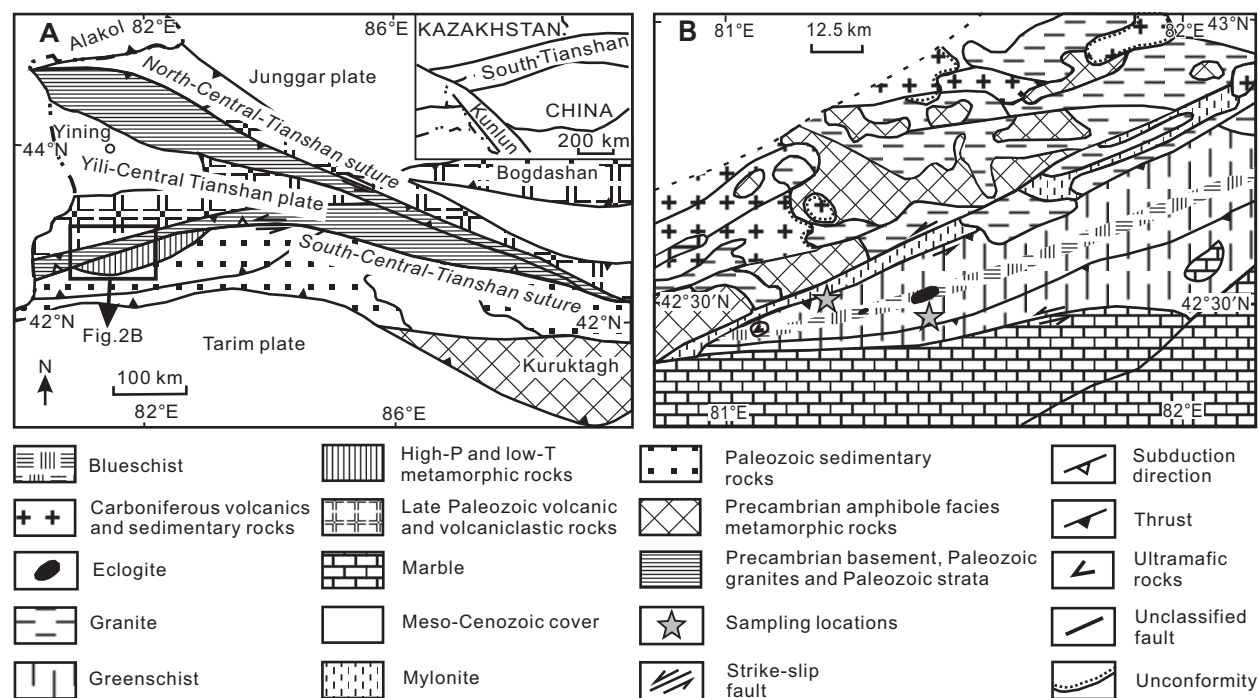


**Figure 2.** Simplified map of Chinese western Tianshan Mountains (after Gao and Klemd, 2003; Zhang et al., 2003). (A) Geological map for the location of western Tianshan. (B) Distributions of our sampling positions.

2005) to argue against the UHP metamorphism. One reason to accept the calculated pressures against the observation of coesite in these rocks (Zhang et al., 2005) is that these authors did not find coesite in samples they studied. Coesite is volumetrically rare, and it can be widespread throughout an UHP metamorphic belt, but it is not necessarily present in every random sample. For example, if we make 10 thin sections from a single hand specimen, we may not find coesite at all or may find coesite only in one of the 10 thin sections. This is also the reason why it may take a long time to confirm one UHP metamorphic belt. It is thus incorrect to argue that the thin section that contains coesite had subducted to depths >80 km while the other nine thin sections of the same hand specimen without coesite had not subducted to that depth. Furthermore, because of the rapid subduction and exhumation, the rock may not stay at peak  $P$ - $T$  conditions long enough relative to the quartz-coesite transformation, which can result in even rarer occurrence of coesite. In addition, because of the widespread retrograde metamorphism and overprints, it is also likely that coesite crystals may have completely reverted to quartz during reequilibrium at lower pressures.

Although not observed in samples we studied, previous studies identified other lines of evidence for UHP metamorphism in western Tianshan, e.g., the presence of quartz and coesite exsolution lamellae due to decompression of

the Ca-Eskola ( $\text{CaEs-Ca}_{0.5}\text{AlSi}_2\text{O}_6$ ) component in omphacite of Tianshan eclogites (e.g., Zhang et al., 2002a), and the coexistence of dolomite, magnesite, and calcite (aragonite pseudomorph) in rocks of sedimentary protolith within Tianshan eclogite bodies (e.g., present between eclogitized basaltic flows and pillows; Zhang et al., 2002b, 2003). The latter two arguments, however, are not definitive evidence for UHP metamorphism. For example, Ca-Eskola could be stable in the quartz (vs. coesite) stability field (Page et al., 2005), and the decomposition of dolomite may take place at lower pressures (e.g., 2.3–2.8 GPa; Smit et al., 2008). Nevertheless, the presence of coesite, together with the arguments considering Ca-Eskola composition and dolomite decomposition, ~2.5 GPa is likely the minimum for peak pressure. Hence, there should be no dispute on the occurrence of UHP metamorphism in western Tianshan.

## PETROGRAPHY

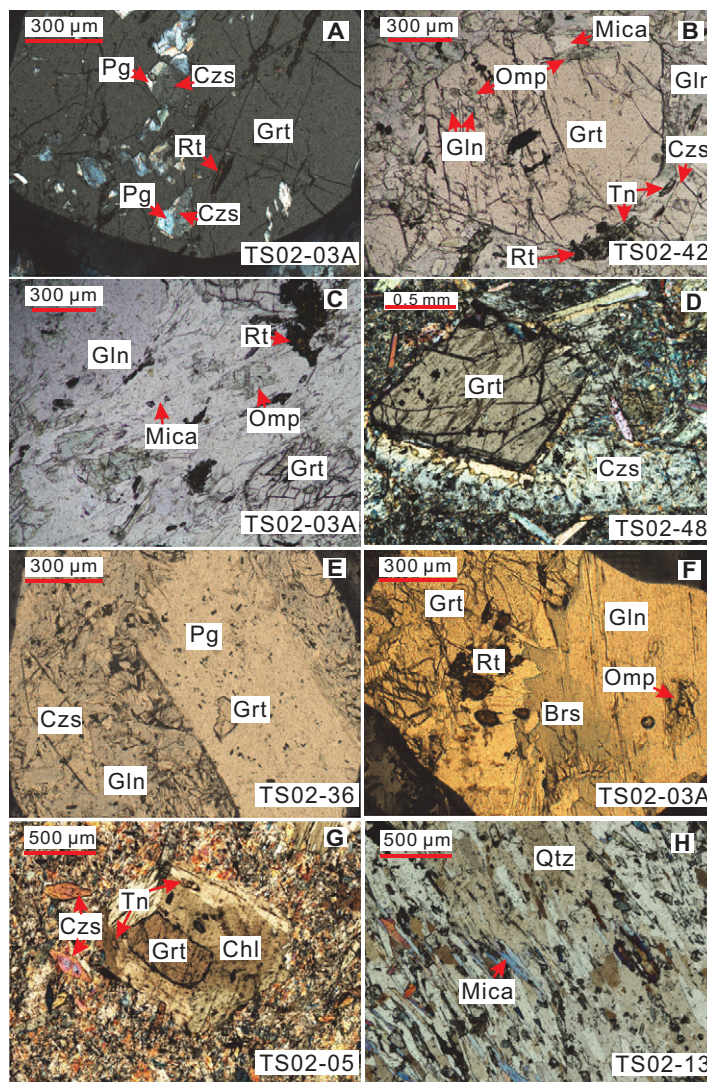
The UHP metamorphic belt in Tianshan is dominated by blueschist and eclogite pods and lenses, surrounded, in fault contacts, by greenschist-facies rocks (Fig. 2). In total, 50 samples were taken from locations broadly similar to those reported by Gao and Klemd (2003) and Zhang et al. (2003), including one rodingite TS02–34, which is dominantly made up of garnet (69.4 vol%). An additional nine samples

were provided by Lifei Zhang from localities described in Zhang et al. (2003). Detailed petrography is given in Table DR1.<sup>1</sup> Rocks of sedimentary protolith (Fig. 3H) can be readily distinguished from rocks of basaltic protolith (Figs. 3A–3G; some of which are sampled from the well-preserved pillows in the field) by their very high modal abundances of quartz and carbonate, as well as more obvious foliations defined by high modes of white mica and relatively low modes of (clino)zoisite. Many samples of sedimentary protolith have ~50 vol% quartz, and these are termed as quartz mica schists (Fig. 3H; Table DR1 [see footnote 1]). Compared with rocks of basaltic protolith, rocks of sedimentary protolith tend to show stronger retrogressive overprints, particularly the extent of chloritization of minerals such as garnet and white mica.

Samples TS02–3B, TS02–15A, TS02–17b, and TS02–32A belong to typical eclogite (where garnet + omphacite > 70 vol% of the bulk rock). They are composed of garnet porphyroblasts and fine-grained omphacite matrix, along with varying amounts of accessory minerals, including amphibole (Na-amphibole with a little [sodic-]calcic amphibole), (clino)zoisite,

<sup>1</sup>GSA Data Repository item 2012136, Tables DR1–DR6 and Figure DR1, is available at <http://www.geosociety.org/pubs/ft2012.htm> or by request to [editing@geosociety.org](mailto:editing@geosociety.org).

**Figure 3.** Photomicrographs of representative samples from western Tianshan. (A–G) Samples of basaltic protolith from group 1 (see Table DR1 for classifications [see text footnote 1]) and (H) one sample of sedimentary protolith. (A) Eclogitic blueschist. Coexisting paragonite and clinozoisite preserved as tabular inclusions in garnet poikiloblast may represent lawsonite pseudomorphs. (B) Eclogitic blueschist. Idioblastic garnet with omphacite and glaucophane inclusions indicates a prograde blueschist-facies metamorphism. In the lower-right corner of this photo, rutile has been replaced by surrounding titanite during retrograde metamorphism. (C) In samples dominated by glaucophane, the presence of white mica and omphacite inclusions indicates that the glaucophane in this sample, TS02-03A, was produced by retrograde metamorphism rather than prograde metamorphism. This retrograde sample is used in later sections for discussing rehydration effects on reenrichment, compared with eclogite TS02-03B. (D) Omphacite-garnet epidosite. One idioblastic garnet grain has grown at the expense of prograde clinozoisite nearby, resulting in a resorption grain boundary at the rim of the latter. (E) Epidote blueschist. Garnet inclusion in the paragonite probably reflects a reenriched process caused by rehydration during retrograde metamorphism. (F) Glaucophane has barroisite overgrowth at rim, one omphacite inclusion as well, caused by retrograde overprints. (G) Epidote-bearing blueschist with chlorite overprinting on garnet porphyroblast. (H) Chloritized quartz mica schist, characterized by abundant quartz and foliation fabrics. B–C and E–F were taken under plane polarized light (PPL); others were taken under crossed polarized light (XPL). The mineral abbreviations used in this paper are: Ab—albite; Act—actinolite; Ae—aezgirine; Alla—allanite; Amp—amphibole; Ang—antigorite; Arg—aragonite; Brs—barroisite; Ca—carbonate; Chl—chlorite; Cld—chloritoid; Czs—clinozoisite; Cpx—clinopyroxene; Di—diopside; Dol—dolomite; Epi—epidote; Gln—glaucophane; Grt—garnet; Horn—hornblende; Jd—jadeite; Law—lawsonite; Mag—magnesite; Mica—white mica (including both phengitic muscovite and paragonite); Omp—omphacite; Qtz—quartz; Pg—paragonite; Phen—phengitic muscovite; Prp—pyrope; Rt—rutile; Tn—titanite; Tr—tremolite; and Zs—(clino)zoisite.



white mica (both phengitic muscovite and paragonite), rutile, titanite, quartz, and carbonate. Glaucophane and omphacite inclusions in garnet indicate that eclogites underwent a prograde blueschist-facies metamorphism prior to reaching the eclogite facies, i.e., stage 1 in Figure 4. Glaucophane also occurs as discrete relicts of prograde metamorphism in the matrix, and only some of them show the overgrowth of (sodic-)calcic amphibole on glaucophane (e.g., TS02-15A), indicating a highly progressive metamorphism and limited retrograde metamorphic overprints. The relatively low modal (clino)zoisite (no more than 1.07 vol%) may be attributed to less retrograde (clino)zoisite formation and more pronounced breakdown of prograde (clino)zoisite evidenced by resorption features (Fig. 3D; John et al., 2008), representing stage 2 in Figure 4.

Blueschist is dominated by glaucophane and (clino)zoisite with or without omphacite.

(Clino)zoisite could be locally abundant (up to 20 vol%), forming omphacite-garnet epidosite. Glaucophane, omphacite, white mica, (clino)zoisite, carbonate, and quartz are also typical inclusions in garnet poikiloblasts (e.g., Figs. 3A–3B). An observation of particular note is the occurrence of (clino)zoisite and paragonite preserved as inclusions in garnet, forming box-shaped lawsonite pseudomorphs (e.g., Fig. 3A; this is also observed in eclogites) and suggesting a previous lawsonite-bearing blueschist-facies metamorphism, i.e., stage 1 in Figure 4.

In addition to evidence for prograde metamorphism afforded by mineral inclusions in garnet, prograde (clino)zoisite also shows amoeboid grain boundaries caused by replacement of omphacite (also see fig. 5 in John et al., 2008). The presence of prograde (clino)zoisite in the lawsonite stability field may result from the relatively low  $H_2O$  content in the system (Poli and Schmidt, 1997). Prograde white micas are also

present (e.g., as inclusions in glaucophane in Fig. 3C), which, together with prograde (clino)zoisite, may also reflect stage 1 conditions (Fig. 4). Sample TS02-01, a chloritoid-bearing omphacitic-epidosite (not shown in Table DR1) has chloritoid poikiloblasts, which contain glaucophane, idioblastic (clino)zoisite, and white mica inclusions, and indicate the transition from stage 1 to stage 2 in Figure 4.

Idioblastic retrograde (clino)zoisite and retrograde white micas (e.g., one paragonite porphyroblast, including one garnet relict, in Fig. 3E) are also present, representing stage 3 in Figure 4. (Sodic-)calcic amphiboles are common, most of which have clearly replaced other minerals like garnet. Clear zonings, e.g., (sodic-)calcic amphibole having Na-amphibole cores (reflecting stage 5 in Fig. 4), and even containing omphacite inclusions (e.g., Figs. 3C and 3F reflecting stage 4 in Fig. 4), indicate retrograde metamorphism from eclogite to (epidote-) amphibolite facies.

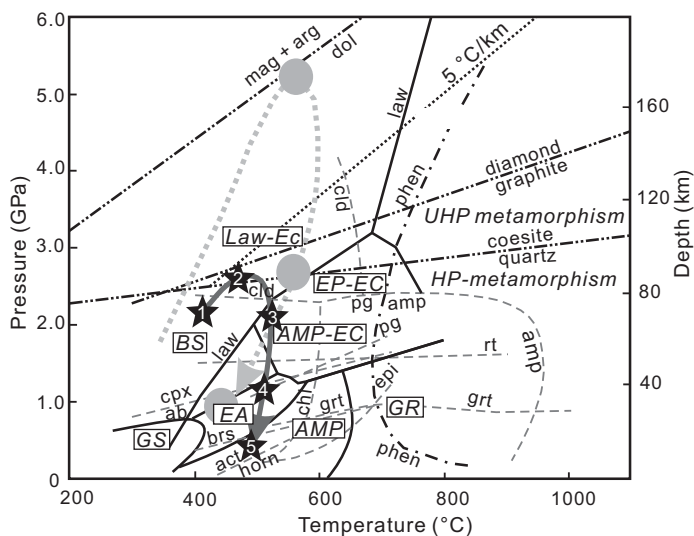


**Figure 4.** Schematic phase diagram after El Korh et al. (2009), Schmidt and Poli (1998), Poli and Schmidt (2002), and Zhang et al. (2003). Abbreviations: GS—greenschist; BS—blueschist; EA—epidote amphibolite; AMP—amphibolite; EC—eclogite; GR—granulite; other abbreviations are given in the caption of Figure 3. The light-gray dotted curve with solid circles is the pressure-temperature ( $P$ - $T$ ) path for western Tianshan reported by Zhang et al. (2003). The dark-gray curve with stars is a schematic  $P$ - $T$  path for our samples based on detailed petrography, with the peak metamorphic condition chosen following Lü et al. (2009). Each numbered star represents one crucial step (i.e., “stage x” mentioned in the text) evidenced by different mineral assemblages and characterized by index minerals.

This is also reflected by the development of titanite at the rims of rutile (e.g., Fig. 3B). Carbonate is common and can be abundant (Table DR1 [see footnote 1]). Some carbonate minerals are well crystallized, showing an equilibrium texture with coexisting silicate phases, reflecting their protolith inheritance and metamorphic recrystallization. However, retrograde carbonate also occurs as irregular patches or fine veinlets replacing other minerals (including garnet).

All the foregoing petrographic observations formed the basis for the schematic  $P$ - $T$  path to illustrate the concept (Fig. 4), although individual samples are likely to have undergone different extents of retrograde metamorphism. The peak metamorphic  $P$ - $T$  conditions we considered here are the corrected estimates of Lü et al. (2009), i.e., 470–510 °C at 2.4–2.7 GPa.

## ANALYTICAL METHODS

Abundances of both major and trace elements in bulk-rock samples were measured at Cardiff University. An Ultima 2 inductively coupled plasma–optical emission spectrometer (ICP-OES) was used for the major-element analyses and a Thermo Element-x7 series quadrupole

inductively coupled plasma–mass spectrometer (ICP-MS) was used for the trace-element analyses. Hand specimens were first processed using a diamond wheel to remove saw marks and weathered surfaces before being rinsed with deionized water. The dried samples were then crushed using a clean jaw crusher and powdered with either an agate Tema mill or agate ball mills.

To ensure high-quality data, complete sample dissolution, especially for refractory minerals such as zircon and rutile, is essential (e.g., Yu et al., 2001). We chose two methods: lithium metaborate fusion for most elements (by which zircon, rutile, titanite, etc., are readily dissolved; e.g., Yu et al., 2001), and HF-HNO<sub>3</sub> dissolution of sample powders for Pb, low-abundance elements, and elements that are not analyzable in LiBO<sub>2</sub>-fused solutions (such as Cs because of its volatility). Through comparisons with Ultrapure SPEX CertiPrep 100% lithium metaborate, Spectroflux ultraclean 100% lithium metaborate was the best flux in the LiBO<sub>2</sub>-fused solution method because of its lower Nb content. In the second method, routine HNO<sub>3</sub> washing was used to wash laboratory instruments and flush the instrument between analysis runs. Additional flushing of the instrument with HCl was

also used to remove Pb from the sample lines. We used JB-1a (a Geological Survey of Japan basalt reference rock standard) as an unknown monitor (Table DR2; Ando et al., 1987). The precision and accuracy for all the analyzed trace elements are, respectively, within 5% and ±10% uncertainties (see Table DR2 [see footnote 1]).

Mineral compositions were analyzed using a Cambridge (Leo) S360 scanning electron microscope (SEM) at Cardiff University equipped with an INCA<sup>®</sup> energy dispersive X-ray spectrometer (EDS) of Oxford Instruments monitored with a Co standard. The beam current was ~1 nA, and the accelerating voltage was 20 kV. Analyses were conducted with 50 s counting time and 45% dead time for optimizing the signals. Generally, the detection limits are better than ~0.03% and 0.02% (equivalent to 2σ), respectively, for elements in silicate phases and base metals in sulfides (Peter Fisher, 2011, personal commun.). Data reduction was done using ZAF correction with INCA Energy + software. Natural and synthetic standards from Micro-Analysis Consultancy Ltd. were used for calibrations. Garnet, omphacite, amphibole, white mica, and epidote group minerals were analyzed quantitatively. Representative mineral analyses and formula calculations are given in Table DR3 (see footnote 1). All these data were reported by Lavis (2005).

## MINERALOGY AND BULK-ROCK COMPOSITION

### Mineral Compositions

Garnet shows a sharp compositional variation, with increasing pyrope composition at the rims in most samples (Table DR3 [see footnote 1]). Clinopyroxene is omphacitic (Fig. 5A; Table DR3 [see footnote 1]). Amphiboles vary in composition, from typical glaucophane to calcic and sodic-calcic amphiboles including actinolite, barroisite/katophorite, and magnesiohornblende (Fig. 5B). Representative analyses of specific types of amphiboles are given in Table DR3 (see footnote 1). Both phengitic muscovite and paragonite mica exist (Table DR3 [see footnote 1]), and are classified in terms of K/Na ratio. Compositions of epidote group minerals are also variable, especially in total FeO (Table DR3 [see footnote 1]).

### Major-Element Analyses and Reconstructed Bulk-Rock Composition

Table DR4 (see footnote 1) shows bulk-rock major- and trace-element contents. Samples of sedimentary protolith have variably high SiO<sub>2</sub> (52.09–76.66 wt%) and relatively low MgO

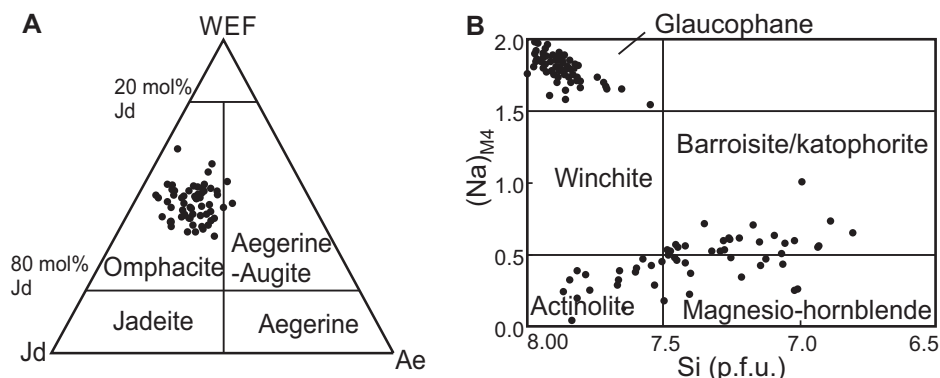


**Figure 5.** Compositional classification of clinopyroxene and amphibole. (A) WEF (wollastonite + enstatite + ferrosilite)-Jd-Ae diagram following Morimoto (1988) for clinopyroxene compositions, all of which have omphacitic compositions. (B)  $(\text{Na})_{\text{M4}}-\text{Si}$  (p.f.u.) diagram for amphiboles (Leake et al., 1997), showing compositional distinctions between glaucophane and other amphiboles.

(1.81–4.82 wt%), CaO (1.29–7.67 wt%), and  $\text{TiO}_2$  (i.e., <1.13 wt%). Samples of basaltic protolith have low  $\text{SiO}_2$  (40.96–53.19 wt%) and  $\text{Al}_2\text{O}_3$  (<20 wt%) and relatively high MgO (up to 8.56 wt%). Major elements are highly variable, including loss on ignition (LOI), which is closely associated with the estimated carbonate modal abundances evidenced by their significant correlations (not shown). The pronounced high carbonate modal abundances in several samples also explain the high CaO and low  $\text{SiO}_2$  contents (e.g., TS02-06, 106–14). Among different groups of samples of basaltic protolith (see the following section for classification), group 1 generally has the highest  $\text{TiO}_2$  (1.62–3.85 wt%) and  $\text{K}_2\text{O}$  (up to 3.63 wt%). Group 2 shows the lowest  $\text{TiO}_2$  (<2 wt%), except for two samples (TS02-15A and TS02-15B), which have major compositions distinctive from other samples of the same group, i.e., much higher  $\text{TiO}_2$  (2.78 and 2.80 wt%) but lower Mg# (31.10 and 32.19). One sample of ultramafic protolith (TS02-34) contains only 34.01 wt%  $\text{SiO}_2$  and low Mg# (i.e., 20.44).

To understand the redistribution of elements (including flux in and out of the system) between mineral phases in our subsequent studies using in situ major- and trace-element analyses, it is necessary to perform a quantitative analysis of mineral modes. Detailed modal analyses of these rocks were done by point-counting using a James Swift automatic point counter, model F 415C. The modal data are given in Table DR1 (see footnote 1). Comparisons of reconstructed bulk-rock major-element compositions (the calculation method and the calculated results are given in the caption of Fig. DR1 [see footnote 1]) with actual analyses indicate that our estimations of mineral modes are reliable (Fig. DR1

[see footnote 1]), although some uncertainties still exist (see discussions in the caption of Fig. DR1 [see footnote 1]).

#### TRACE-ELEMENT MOBILITY AND GEOCHEMISTRY OF SAMPLE GROUPS

##### Sample Grouping

Experimental studies (e.g., Manning, 2004; Kessel et al., 2005; Hermann et al., 2006) have shown that high field strength elements (HFSEs, i.e., Ti, Zr, Hf, Nb, Ta) together with Y and the middle to heavy rare earth elements (M-HREEs), are usually not mobile during fluid-rock interactions. These studies also show that Th and LREEs are usually immobile. Alkali and alkali earth elements such as Rb, Cs, and Ba are usually mobile, as are Na and K, used for the classification of modern lavas. For this reason, immobile elements should be used for rock classification and tectonic discrimination of protoliths of metamorphic rocks (e.g., Pearce and Cann, 1973; Winchester and Floyd, 1977).

The Zr/Ti versus Nb/Y diagram (Winchester and Floyd, 1977) is often used as an immobile trace-element equivalent of the TAS (total alkali vs. silica) diagram to classify volcanic rocks with varying degrees of alteration/metamorphism in the geological records. In Figure 6A, which uses the updated boundaries of Pearce (1996), samples of basaltic protolith plot in three clusters, mainly in the subalkalic basalt field. They display a small range in Zr/Ti ratio (equivalent to a small  $\text{SiO}_2$  variation) but a large range in Nb/Y ratio (equivalent to large total alkali variations). We term these group 1, group 2, and group 3 samples, respectively (see

Tables DR1 and DR4 [see footnote 1] for mineral assemblages and geochemical data).

Provided that Th, Nb, Ti, and Yb are immobile throughout the metamorphic process, the Th/Yb versus Nb/Yb and Ti/Yb versus Nb/Yb diagrams (Pearce, 2008) are effective in fingerprinting tectonic settings of magma eruption. The first of these diagrams features a diagonal MORB-OIB array containing N-MORB, E-MORB, and OIB compositions (Fig. 6B). Basalts with a subducted or assimilated continental crustal component plot above this array; these include volcanic arc basalts, some back-arc basin basalts, and basalts contaminated with continental crust materials. For our samples, the three groups defined in Figure 6A are also well separated on this projection. Samples from group 1 and group 3 plot within or at the field edge of the MORB-OIB array. Their protoliths are most likely OIB- or E-MORB-like and depleted MORB-like rocks, respectively. The high Ti/Yb ratios of the former on the Ti/Yb-Nb/Yb diagram (not shown) demonstrate that these are OIB-like rather than E-MORB-like.

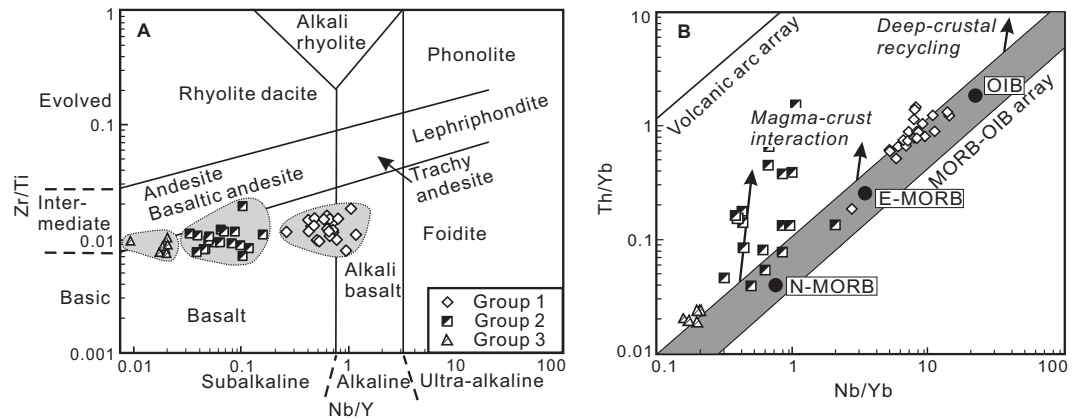
In contrast, group 2 samples define a distinct trend away from the MORB-OIB array into the volcanic arc/contamination field. Because this trend includes samples within the MORB-OIB array, it is likely to reflect the effect of crustal contamination of MORB-like magmas or a mixing relationship between MORB and arc magmas (Pearce, 2008). Group 2 samples will be excluded from the study of element mobility (see following) because alteration and contamination (or mixing) effects cannot be easily resolved in the bulk-rock studies.

##### Determination of Element Mobility or Immobility

Although HFSEs and HREEs have been widely considered to be immobile, there is some evidence that they are not always conserved during subduction-zone metamorphism (e.g., Gao et al., 2007; John et al., 2008), which is possible in the case of some subduction-zone fluids (e.g., supercritical  $\text{H}_2\text{O}$ -rich fluids,  $\text{CO}_2$ -rich fluids, and perhaps, even  $\text{SiO}_2$ -rich hydrous melts; Manning, 2004; Kessel et al., 2005). Therefore, to understand the geochemical consequences of subduction-zone metamorphism properly, it is necessary to examine the actual mobility and immobility of each element of geochemical significance in our samples.

Because elemental behavior during the formation of igneous protoliths is governed by the partition coefficient during partial melting/crystallization, elements with similar incompatibility in igneous protoliths are expected to be significantly correlated. Based

**Figure 6.** (A) Zr/Ti-Nb/Y diagram for rocks of basaltic protolith (after Winchester and Floyd, 1977; Pearce, 1996). (B) Th/Yb versus Nb/Yb for rocks of basaltic protolith (after Pearce, 2008). Ocean-island basalt (OIB), enriched (E)-, and normal (N) mid-ocean-ridge basalt (MORB) are plotted for comparison (black solid circles; the values of oceanic basalts are from Sun and McDonough, 1989).



on this principle, one simple way to examine the element mobility or immobility is to see if these statistically significant correlations are preserved (or not) in our metamorphic samples, i.e., whether these elements have been fractionated from each other during metamorphism (e.g., Niu, 2004). If a significant correlation between two similarly incompatible elements is preserved in the metamorphic rocks, then these two elements have remained immobile; otherwise, one of them or both may have been mobilized during metamorphism. Note that two mobile elements with similar incompatibility may also exhibit significant correlations. Therefore, we selected two HFSEs with different incompatibilities (i.e., Nb and Zr) and investigated their correlations with other trace elements with varying incompatibility, i.e., Nb with large ion lithophile elements (LILEs), LREEs, Th, U, and Ta, and Zr with MREEs, some LREEs, and Hf (Fig. 7).

Investigations of correlation coefficients were carried out following the methods of Niu (2004) and Lavis (2005) for cogenetic rocks of basaltic protolith from group 1 (Figs. 7A–7B) and group 3 (not shown), and for rocks of sedimentary protolith in Table DR5 (although the method is less effective in metasedimentary rocks than for metabasaltic rocks; see footnote 1). Figure 7 shows the correlation coefficients of the immobile incompatible elements Nb and Zr with other trace elements, which are sorted in order of decreasing incompatibility from left to right following the order reported by Niu and Batiza (1997). For  $N = 23$  (group 1) and  $N = 6$  (group 3), only those correlations above 0.482 and 0.882, respectively, are treated as statistically significant correlations at >99% confidence levels. In Figure 7, we find that Ba, Cs, Rb, K, Pb, and Sr are not significantly correlated with Nb and Zr and have, therefore, been mobilized in our samples of basaltic protolith, during either prograde or retrograde metamorphism (i.e.,

during seafloor alterations). All other elements showing statistically significant correlations with Nb and Zr (i.e., REEs, HFSEs, Th, and U) have thus remained largely immobile.

Previous studies (e.g., John et al., 2004) showed that LREEs, U, and Th can be fractionated from HFSEs and HREEs during subduction-zone metamorphism. However, Figure 8E shows that the U/Nb ratio of our samples is constrained within a small range similar to that of N-MORB, except for samples from group 2 that have been attributed to the contamination or mixing with materials with high, possibly variable, U/Nb ratios, such as continental crust (see previous). In addition, Nb/La ratios of our samples are also relatively constant, i.e.,  $0.94 \pm 0.15$

( $1\sigma$ ; group 1) and  $0.45 \pm 0.06$  ( $1\sigma$ ; group 3). Together with the significant linear correlations between U and Th (Fig. 8F), all these values suggest that U, Th, and LREEs in our samples have not been mobilized since the formation of their protolith, as predicted for HFSEs and HREEs. Furthermore, the compositional range of altered ocean crust is relatively large with respect to U content, which may be enriched by up to five times in altered ocean crust, as shown in the super-composite composition of the tholeiitic section of ocean crust in Ocean Drilling Program Site 801 (Kelley et al., 2003), and U shows its strong mobility during seafloor alteration (also see Niu, 2004). Thus, altered ocean crust may show a poor correlation of U with

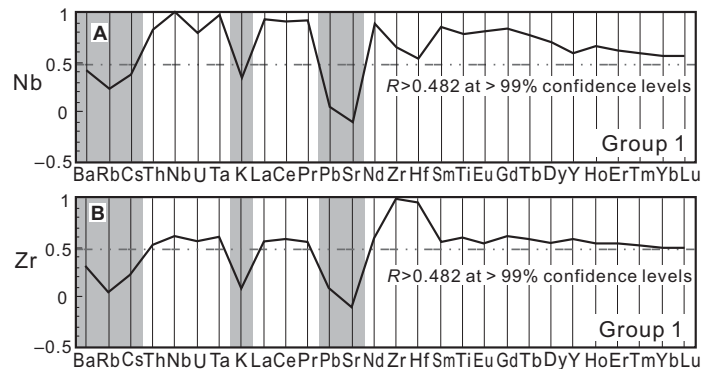
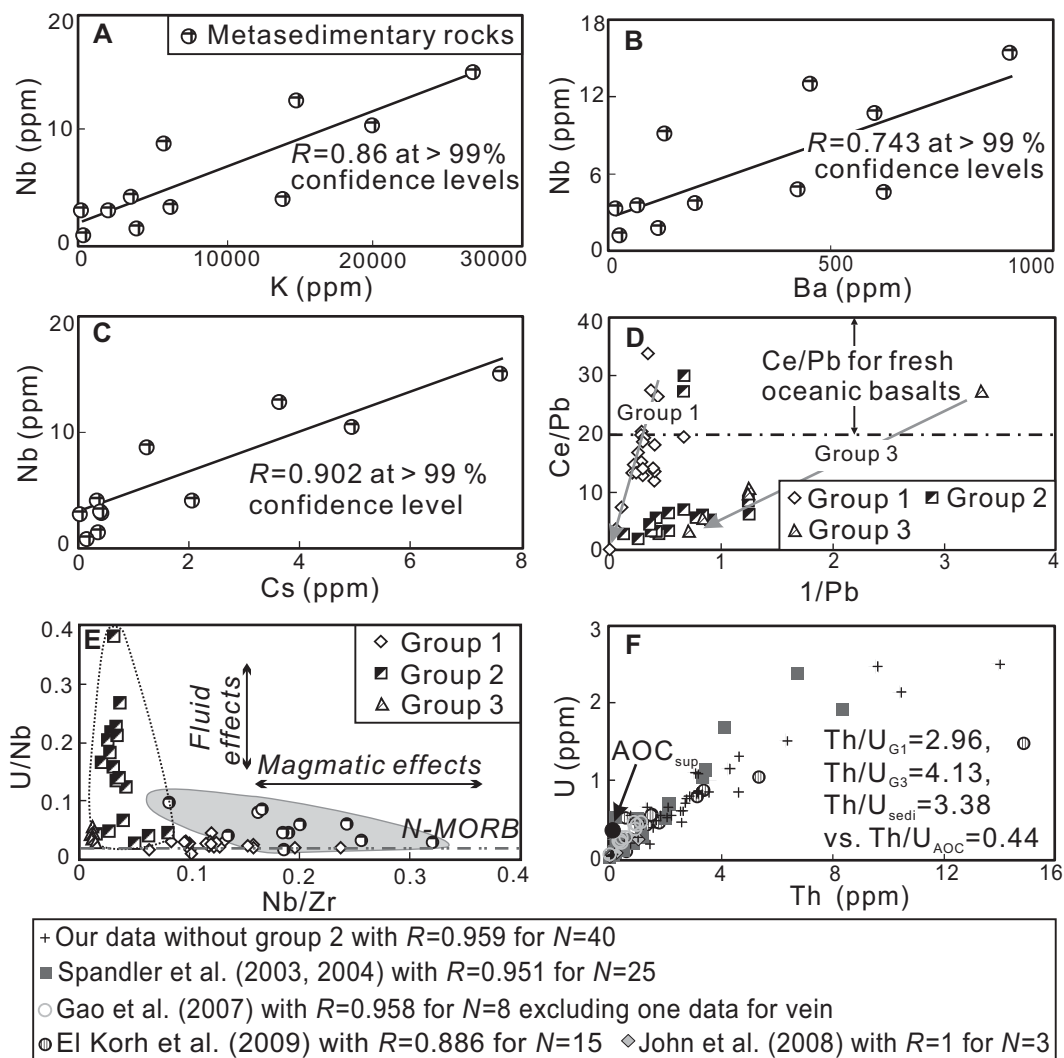


**Figure 7.** Correlation coefficient diagrams of Nb (A) and Zr (B) with other trace elements for samples of group 1 from western Tianshan (Niu, 2004; Lavis, 2005). Elements along x-axis are ordered in terms of decreasing incompatibility from left to right. Two immobile elements (Nb and Zr) were chosen considering their different incompatibility; therefore significant correlation coefficients with Nb or Zr can reflect immobility of elements with varying incompatibility. The dashed lines represent the minimum significant correlation coefficient, i.e., 0.482 (refer to critical value of Pearson's correlation coefficient using a one-tail test) at 99% confidence levels for 23 samples (i.e., the degree of freedom is 21). Similar conclusions can also be made for samples from group 3.

**Figure 8. Covariation diagrams.** (A–C) Statistically significant (at >99% confidence levels; the critical value of Pearson's correlation coefficient using one-tail test for 11 samples is 0.685) correlations of large ion lithophile elements (LILEs) with Nb in rocks of sedimentary protolith, suggesting relative immobility of K, Cs, Ba, and Rb (not shown here) during subduction-zone metamorphism. (D) Ce/Pb versus 1/Pb for rocks of basaltic protoliths (after John et al., 2004). The Ce/Pb range for fresh oceanic crust is from Bebout (2007). Gray arrows indicate the trend of the Pb addition for group 1 and group 3. (E) U/Nb versus Nb/Zr for rocks of both sedimentary and basaltic protoliths (after John et al., 2004). The U/Nb ratio of normal mid-ocean-ridge basalt (N-MORB) (= 0.02; represented by the horizontal dashed line) is from Sun and McDonough (1989). See the detailed explanation in the relevant text. (F) Correlations between U and Th for rocks of basaltic (group 1 and group 3) and sedimentary protoliths in this study, as well as relevant data in the literature (Spandler et al., 2003, 2004; Gao et al., 2007; John et al., 2008; El Korh et al., 2009), without considering the effect of their different protoliths. The model composition of altered ocean crust (AOC<sub>sup</sub>; super-composite of Ocean Drilling Program Site 801, representing tholeiitic section of ocean crust in Kelley et al., 2003) is also plotted (the black solid circle). The average Th/U ratios of group 1 (Th/U<sub>G1</sub>), group 3 (Th/U<sub>G3</sub>), and metasediments (Th/U<sub>sed</sub>) in this study, and the Th/U ratio of model component of altered ocean crust (Th/U<sub>AOC</sub>) are also given for comparisons. All the U-Th correlation coefficients in the text box beneath the plots are at >99% the confidence levels.



immobile elements (e.g., fig. 4c in Kelley et al., 2005) and have lower Th/U ratios (or Nb/U) in some rocks due to U enrichment. Therefore, the significant linear correlation of U with Th (or Nb, not shown) and the inferred immobility of U, as well as the distinctive Th/U ratios of all our samples from altered ocean crust (Fig. 8F), suggest that the component of altered ocean crust, if involved at all, is insignificant in the protoliths of our samples.

Considering the much lesser mobility of Pb compared with U during seafloor alteration (e.g., Kelley et al., 2005), together with the insignificant effects of seafloor alteration for our samples, it is most likely that the Pb mobility is the result of prograde and/or retrograde metamor-

phism after seafloor alteration, although the mobility of other LILEs (Rb, Cs, and K) may need further studies because of their higher mobility during seafloor alteration. Furthermore, the high Pb contents and low Ce/Pb compared with the range for fresh oceanic crust (see Bebout, 2007) may reflect the addition of Pb (Fig. 8D). As John et al. (2004) suggested, this Pb addition probably happened during exhumation of the slab rocks.

The significant interelement correlations of HFSEs and REEs (Table DR5 [see footnote 1]), and the good correlations of K, Rb (not shown), Cs, and Ba with HFSEs at >99% confidence levels in rocks of sedimentary protolith (Figs. 8A–8C) suggest their rather similar behavior during subduction-zone metamorphism. As HFSEs are

immobile, K, Rb, Cs, Ba, and REEs in samples of sedimentary protolith are also immobile. The poor correlations of Pb and Sr with HFSEs may indicate their mobility during subduction-zone metamorphism. Therefore, based on the previous discussion, Pb and Sr are mobile, while REEs, HFSEs, Th, and U are immobile in both lithologies. The mobility and immobility of K, Rb, Cs, and Ba are protolith dependent, i.e., immobile in rocks of sedimentary protolith but mobile in rocks of basaltic protolith.

Recently, Gao and coworkers (Gao et al., 2007; John et al., 2008) concluded that Nb, Ta, Ti, REEs, and LILEs are all mobile during subduction-zone metamorphism, based on a localized fluid-vein assemblage from western

Tianshan. Although their observations may be valid, we emphasize that caution should be taken not to generalize local phenomena as reflecting the prevailing nature of subduction-zone metamorphism. Our data demonstrate clearly that REEs and HFSEs are largely, if not entirely, immobile during subduction-zone metamorphism (Figs. 7–8).

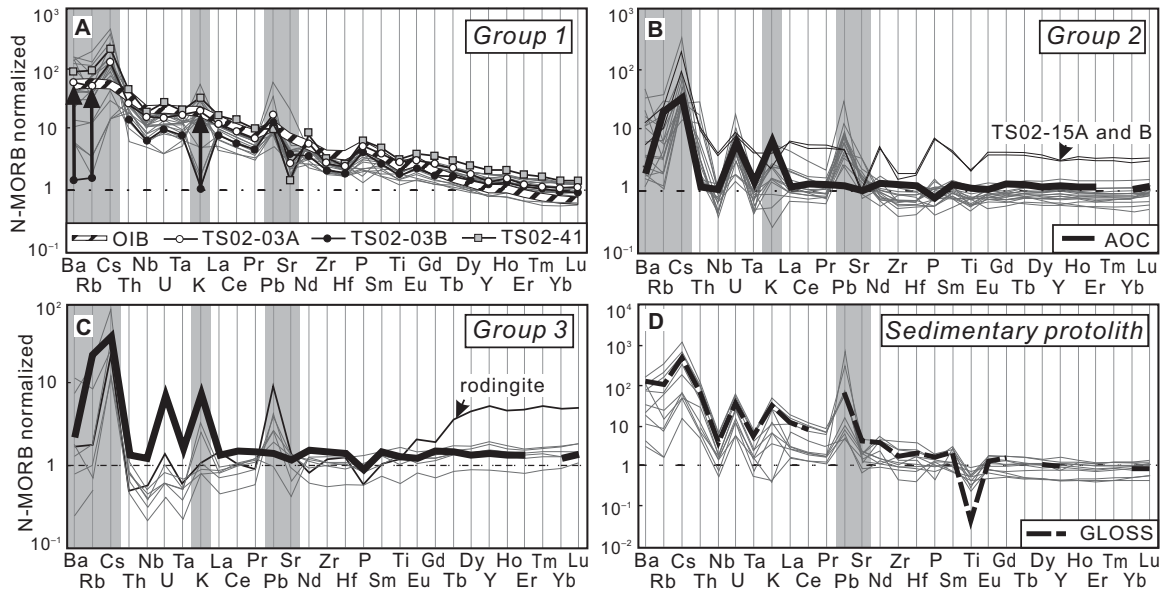
### Geochemistry of Different Sample Groups

Figure 9 shows N-MORB normalized multi-element diagrams for rocks of basaltic protolith (Figs. 9A–9C) and for rocks of sedimentary protolith (Fig. 9D). All the mobile elements discussed previously (i.e., LILEs, Pb, and Sr in the gray areas in Figs. 9A–9C) display greater variability than immobile elements due to the “fluid effect” during subduction-zone metamorphism in the case of samples of basaltic protolith. Pb shows obvious enrichment in most samples, which is in correspondence with the previous assumption that Pb addition may occur during retrogressive metamorphism. No obvious Eu anomalies have been found. Mobile elements will not be used in the following discussion on the geochemistry of protoliths and their tectonic settings.

Immobile incompatible elements are generally enriched in group 1, with a pattern similar to the average composition of OIB, which is also consistent with its high  $K_2O$  content. Group 2 displays a relatively flat pattern with stronger enrichments of U and Th relative to Nb and Ta (i.e., higher  $[Th/Nb]_{N-MORB}$  and  $[U/Ta]_{N-MORB}$ ), which are comparable to, or even much higher than (in most samples), the model composition of altered ocean crust (Kelley et al., 2003). Considering the contamination/mixing by continental or arc crustal materials (see Fig. 6B) as well as the insignificant contributions of altered ocean crust (if it is involved at all) in the protoliths (in group 1 and group 3), group 2 protolith may thus likely be derived from an N-MORB-like rock(s) with subsequent continental or arc crust contamination rather than seafloor alterations. Two samples (i.e., TS02–15A and TS02–15B) from group 2 (Fig. 9B) show overall elevated trace-element abundances and lower Mg# (Table DR4 [see footnote 1]), which are consistent with the protolith being more evolved basalts. Samples from group 3 are depleted in the progressively more incompatible elements and enriched in the less incompatible elements (such as HREEs), indicating a pattern similar to that of highly depleted MORB-like basalts (Fig. 9C).

As discussed already, LILEs are considered as immobile elements in rocks of sedimentary protolith; therefore, the large concentration range of LILEs shown in Figure 9D is inherited from the compositional heterogeneity of sedimentary protolith, rather than the mobility of LILEs. In contrast, variations in Pb and Sr concentrations are most likely attributed to their fractionations owing to their mobility. Most samples of sedimentary protolith have similar compositions to global oceanic subducted sediments (GLOSS; Plank and Langmuir, 1998) with enriched LILEs and depleted HFSEs, while those depleted in LILEs are likely rocks of graywacke protolith with arc-basalt contributions.

Considering both the field study in western Tianshan (e.g., Volkova and Budanov, 1999; Ai et al., 2006) and the geochemical variability of modern seamounts from enriched OIB-like to depleted MORB-like basalts (such as those near East Pacific Rise seamounts; Niu and Batiza, 1997), we suggest that the UHP metamorphic rocks from western Tianshan may have resulted from the subduction and exhumation of a tectonic mélange that was composed of normal seafloor with dismembered seamounts, sediments, and volcanic arc-derived materials.



**Figure 9.** Normal mid-ocean-ridge basalt (N-MORB) (Sun and McDonough, 1989) normalized multi-element diagrams of different groups for samples of basaltic protolith (A–C) and sedimentary protolith (D), following the decreasing order of elemental incompatibility determined by X/Y-X plots (Niu and Batiza, 1997). Average ocean-island basalt (OIB) (A; Sun and McDonough, 1989), the model composition of altered ocean crust (B–C; super-composite of Ocean Drilling Program Site 801, representing tholeiitic section of ocean crust in Kelley et al., 2003), and global oceanic subducted sediments (GLOSS) (D; Plank and Langmuir, 1998) are plotted for comparison. Three representative samples are also highlighted in Figure 9A, and the vertical arrows represent the effect of re-enrichment caused by rehydration during retrograde metamorphism. Elements in light-gray areas are generally mobile as discussed in previous text.

## DISCUSSION

## Constraints on Trace-Element Budgets

## General Thoughts

In the standard model of subduction-zone metamorphism, the transition from blueschist to eclogite facies was thought to mark the major dehydration reaction within the subducted ocean crust (e.g., Peacock, 1993; Liu et al., 1996). However, in recent studies (e.g., Spandler et al., 2003, 2004), it has been proposed that this transition does not necessarily result in the liberation of mobile elements with released fluids. This is consistent with the poor correlations of fluid-soluble element contents with the glaucophane modal abundance (Fig. 10H), which could reflect the extent of eclogitization, i.e., the main dehydration process. Furthermore, considering the significant contribution of carbonate to LOI and its important influence on major elements in bulk-rock compositions, the lack of an obvious relationship between carbonate mode and Sr (the expected preferential element in carbonate) may reflect the much lesser significance of carbonate to affect the migration of these trace elements, or it may be caused by the occurrence of different carbonate generations (Fig. 10D).

Observations and experimental studies of hydrous minerals (e.g., phengite, lawsonite, [clino]zoisite and allanite) under subduction-zone conditions (e.g., Pawley and Holloway, 1993; Schmidt and Poli, 1998) and studies on the distribution of fluid-soluble elements in different minerals (e.g., Spandler et al., 2003; El Korh et al., 2009) all indicate that these minerals are capable of accommodating fluids in the form of hydroxyl or H<sub>2</sub>O as well as their preferential fluid-soluble elements. Specifically, phengite is the dominant host of K, Rb, Cs, and Ba in the whole rock (e.g., Zack et al., 2001); epidote group minerals (i.e., epidote, [clino]zoisite, and allanite) and lawsonite can host most Sr, Pb, U, Th, and LREEs (e.g., Hermann, 2002; Spandler et al., 2003; Feineman et al., 2007). Therefore, the fluids and the otherwise mobile elements can be carried in the subducting crust (and sediments) for as long and deep as the host hydrous minerals remain stable, e.g., 3.2 GPa for zoisite (~100 km) (even up to 5.0 GPa at 700 °C and 6.6 GPa at 950 °C according to Poli and Schmidt, 1998), up to 12 GPa for lawsonite (~360 km; Schmidt, 1995), and 10 GPa for phengite (~300 km; e.g., Sorensen et al., 1997), and K-hollandite to the deep mantle (i.e., >16–23 GPa for LILEs, Pb, Th, U, and LREEs; Rapp et al., 2008). These depths are far greater than the depth of amphibole stability (commonly 2–2.6 GPa at 700 °C reported by Pawley and Holloway [1993], although it could be stable at higher pressures), and thus those hydrous meta-

morphic minerals that are stable at the UHP metamorphic conditions control fluid-mobile element behavior during subduction-zone metamorphism.

## Constraints on the Budget of LILEs

It is practically not possible to distinguish muscovite and paragonite petrographically unless analyzed grain by grain. Thus, for con-

venience in our modal analyses, these two minerals were considered together as “white mica.” Importantly, our work in progress suggests that both muscovite and paragonite, which occur as solid solutions, have important controls on LILEs, although LILE concentrations in muscovite are about an order of magnitude greater than that in paragonite. Therefore, imprecise identification of muscovite-rich or paragonite-

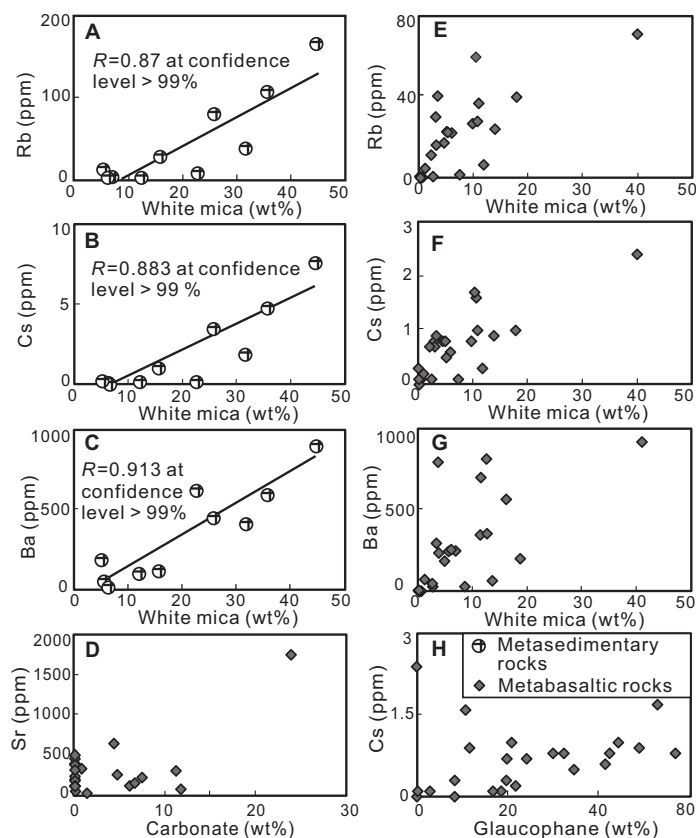


**Figure 10.** Scatter plots of mineral modal abundances with Rb, Cs, Sr, and Ba for (A–C) metasedimentary rocks and (D–H) metabasaltic rocks from group 1 and group 3. (A–C) Statistically significant (at >99% confidence levels) correlations of white mica modes (wt%) with Rb, Cs, and Ba. (E–G) Scattered yet positive trends (statistically insignificant) between white mica modes (wt%) and Rb, Cs, and Ba. (D) Sr shows no obvious trend, with highly variable carbonate content (wt%). Considering the significant contribution of carbonate to loss on ignition (LOI) and the strong capability of carbonate to host and carry Sr (perhaps to a lesser extent Pb and Ba), the absence of correlations between carbonate modal amount and these elements suggests the relatively insignificant effect of carbonate alteration on these elements or presence of different generations of carbonate, which lead to their ambiguous relationship. (H) Plot of glaucophane modal abundance (wt%) against Cs content (ppm). Considering that with stronger eclogitization, glaucophane modes are decreased, the absence of significant correlation of Cs, the mobile element representative, with glaucophane, may reflect that the element mobility is not controlled by the main dehydration during the transition from blueschist to eclogite facies.

rich grains could potentially affect estimated bulk-rock major-element and trace-element concentrations based on mineral modal abundances. We have found, however, that the expected positive trend between white mica modes and the bulk-rock LILE abundances, to a first order, exists in our samples of both sedimentary (Figs. 10A–10C) and basaltic protoliths (Figs. 10E–10G), although correlations of the latter are less significant (see following).

The significant positive correlations of white mica modes with K, Rb, Cs, and Ba abundances in samples of sedimentary protolith (Figs. 10A–10C, not shown for K) indicate that these elements are hosted by white mica as expected. The apparent immobility of these elements in samples of sedimentary protolith discussed previously suggests that white mica, as the primary host of LILEs, may have existed in the protolith and remained stable or recrystallized subsequently during metamorphism. Alternatively, the protolith may have hosted abundant clay minerals with adsorbed K, Rb, Cs, and Ba, and formed white mica in subsequent diagenesis and metamorphism. In any case, the abundances of LILEs in sedimentary protolith remained unaffected by metamorphism because their host minerals have been stable throughout the petrogenetic history of the host rocks.

For rocks of basaltic protolith, there are no significant correlations between white mica modes and Rb, Cs, and Ba (Figs. 10E–10G), suggesting that these elements may not be simply controlled by white mica. Unlike sedimentary rocks, white mica is absent in basaltic protolith, and its presence in rocks of basaltic protolith is of metamorphic origin. Therefore, protolith type and metamorphism both are important in determining the mobility/immobility of LILEs. Given the low concentrations of K, Rb, Cs, and Ba in bulk-rock compositions of average ocean crust (see table 1 in Niu and O'Hara, 2003), little muscovite may be produced from this kind of protolith during metamorphism. Nevertheless, E-MORB- or OIB-like protoliths, or altered ocean crust (see table 6 in Kelley et al., 2003), relatively enriched in  $K_2O$  compared with N-MORB, could supply enough K to produce significant amounts of white mica, which is evidenced by the more common presence of white mica in samples from group 1 (OIB-like source) than in samples from group 3 (depleted N-MORB-like source). On the other hand, the relative timing of white mica formation during metamorphism could also dictate the behavior of those mica-hosted elements. The origin of the poor correlation between LILEs and white mica could have resulted from addition of these elements during retrograde metamorphism (see following discussions), or removal during early

stages of dehydration prior to the crystallization of white mica. However, once white mica has been formed, especially phengitic muscovite, most LILEs will be strongly conserved, and only some LILEs may be lost through the decomposition of phengite at  $>5$  GPa due to the increased potassium solubility in clinopyroxene (Schmidt and Poli, 1998).

#### Constraints on the Budgets of Pb and Sr

Epidote group minerals and their favored trace elements, i.e., REEs, U, Th, Sr, and Pb (e.g., El Korh et al., 2009), are not significantly correlated in metasedimentary rocks, and neither are they correlated in metabasaltic rocks (not shown). Unlike white mica, which is the exclusive host mineral for K, Rb, Cs, and Ba, epidote group minerals are not the sole host for REEs, U, Th, Sr, and Pb (note that the bulk-rock contents of Pb and Sr are not significantly correlated at  $>99\%$  confidence levels). Based on the results in the recent literature (e.g., van der Straaten et al., 2008; Beinlich et al., 2010) and our work in progress on these rocks, Sr (and maybe Pb) can also be accommodated in carbonate and paragonite; REEs can also be incorporated into titanite, as can Sr, Th, U, and Pb to a lesser extent. The influence of these additional phases may therefore explain the observed poor correlations of epidote group minerals with their favored trace elements. Alternatively, considering the immobility of REEs, U, and Th in the bulk rock, the poor correlation is also likely caused by heterogeneous distributions of trace elements in epidote group minerals. In contrast, the poor correlations with Sr and Pb may also reflect the loss/gain of these two elements during the phase transition from lawsonite to epidote or the transition between different epidote generations.

#### Influence of Retrograde Metamorphism

Our samples have generally experienced varying extents of retrograde metamorphism during exhumation. For example, TS02–03A and TS02–03B are different portions of the same hand specimen. The latter sample is a classic eclogite, while the former has retrogressed to a blueschist assemblage with clear retrograde overprints (e.g., Figs. 3C and 3F). Owing to the absence of white mica, TS02–03B is strongly depleted in Rb, Cs, and Ba. However, as the result of localized rehydration, the relatively dry eclogite has been transformed to wet blueschist facies only in TS02–03A. The released K in the fluids (which may be from an external source) led to the formation of higher modal abundance of white mica with high Rb, Cs, and Ba concentrations in TS02–03A, up to  $\sim 100$  times more

enriched than in TS02–03B (as illustrated by the vertical arrows in Fig. 9A). Therefore, in order to understand the actual composition of rocks that have undergone subduction-zone metamorphism (i.e.,  $[P/D]_{out}$ ) and the implications for mantle compositional heterogeneity, we need to evaluate and remove the geochemical effects of retrograde metamorphism first.

Whether the rehydrated rocks will be enriched (i.e., in LILEs, Sr, and Pb) or not during retrograde metamorphism depends on the composition of rocks from which the fluids originated and through which the rising fluids have passed, e.g., enriched OIB- or depleted N-MORB-like basaltic rocks, altered ocean crust, sediments, or within-slab serpentines like “abyssal peridotites” (Niu, 2004).

The serpentinized lithospheric mantle of the subducted slab is one of the most significant fluid reservoirs (e.g., Schmidt and Poli, 1998) for retrograde metamorphism and plays an important role in the exhumation of subducted oceanic lithosphere due to its relatively low density (e.g., Pilchin, 2005). Because of the complex composition of serpentinite-derived fluids, lithologies modified by adding fluids from serpentinite alone may be even more depleted (Fig. 11I). However, considering the enrichment of those retrograde metamorphic rocks (e.g., common enrichment of Pb) and the actual elemental mobility in this study, the depleted fluids derived from serpentines may have scavenged a significant portion of elements from the rocks through which they passed and with which they reacted (e.g., van der Straaten et al., 2008), especially the more enriched rocks such as OIB-like protolith. This suggests that the infiltrated fluids derived from serpentines may be mixed with a subducting sediment- and/or basalt-derived component (the latter is more important for the re-enrichment of Ba, Cs, and Rb in this study; Figs. 11G–11H). Alternatively, fluids derived from rocks that subducted to greater depths than our samples may migrate upward along the subduction channel (Fig. 11G) and could also carry those fluid-soluble elements to metasomatize shallower rocks rather than entering the overlying mantle wedge (Fig. 11H).

#### Implications for Subduction-Zone Magmatism

##### Elemental Contributions to Arc Magmas: LILEs, Sr, and Pb

From the previous discussion, it can be seen that although the transition from blueschist to eclogite facies can theoretically release significant amounts of fluids (Pawley and Holloway, 1993) and fluid-soluble elements for the formation of arc magmas, this may not necessarily

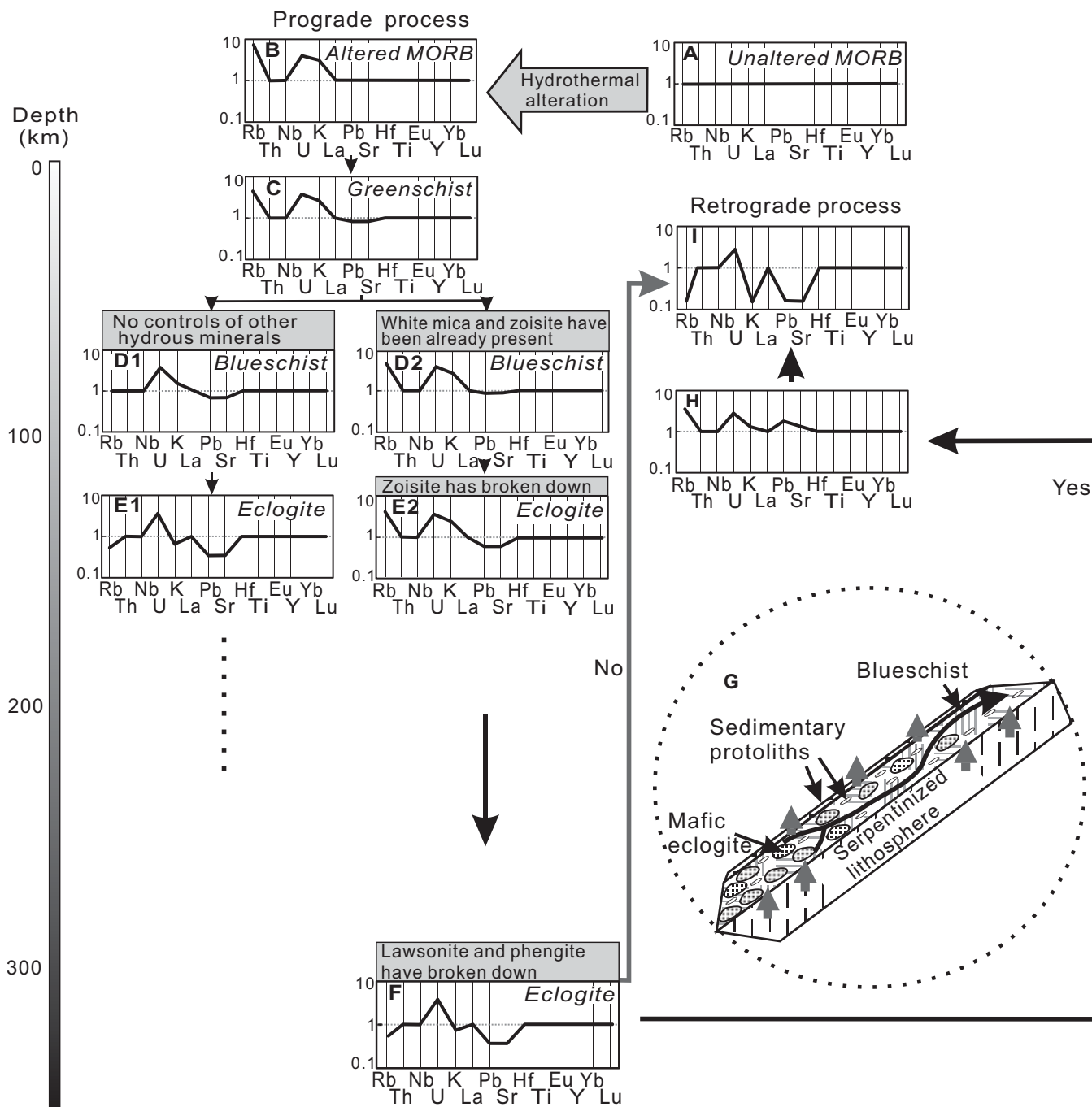
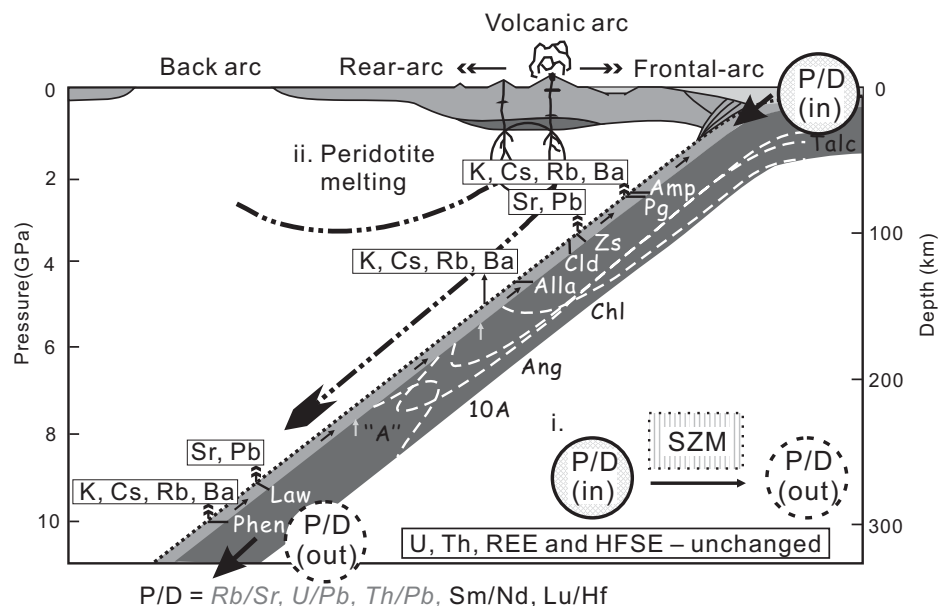


Figure 11. Schematic diagrams showing normal mid-ocean-ridge basalt (N-MORB) normalized trace-element distribution patterns of rocks with theoretical N-MORB composition during hydrothermal alterations (A), prograde metamorphism (B–F), and retrograde metamorphism (G–I) in subduction zones. (D1–E1) Geochemical consequences without considering the presence of hydrous minerals (e.g., phengite, epidote group minerals) that can accommodate mobile elements. In this case, mobile elements (e.g., Cs, Sr, etc.) are released during the blueschist-to-eclogite transition. (D2–E2) The effects of hydrous phases that can retain certain otherwise mobile elements during the blueschist-to-eclogite transition. Considering the actual elemental behavior during subduction-zone metamorphism in this study, F gives the theoretical geochemical consequence at 12 GPa (~360 km), which is the depth at which phengite and lawsonite have broken down. (G–I) The geochemical processes during retrograde metamorphism. Two end-member trace-element distributed patterns (I and H) represent whether the retrograde process may (“yes” path) or may not (“no” path) lead to mobile element enrichment as detailed in G. The widely accepted dehydration of serpentines within mantle sections of the subducted slab may in general represent a “no” path. However, a “yes” path may be followed if the serpentinite-derived fluids could scavenge mobile elements from crustal rocks on their way up. Alternatively, it is also possible that some of the fluids come from dehydration reactions at greater depths within the subducting/subducted rocks (with or without mobile elements) to rehydrate the subducting/subducted rocks at shallow depths, and lead to a “yes” path or a “no” path, respectively.

be the case because some eclogites remain enriched in LILEs, e.g., TS02–41. This highly eclogitized sample without obvious retrograde overprints contains 12.9 wt% white mica and only 0.67 wt% (clino)zoisite, and it has an enriched K-Rb-Cs-Ba and depleted Sr signature without significant Pb enrichment (Fig. 9A). It is white mica that survives from the blueschist-to-eclogite dehydration, retaining/transporting these elements into the deep mantle. Therefore, the appearance and stability of the HP-UHP hydrous minerals (e.g., white mica, [clino]zoisite), which control the immobility/mobility of fluid-soluble elements during subduction-zone metamorphism (the detailed process is illustrated in Figs. 11D–11E), consequently affect the geochemical signatures of arc lavas. Furthermore, it is the major element composition (including H<sub>2</sub>O) and the oxidation state of the protolith that control modal abundances of hydrous minerals at given *P-T* conditions (e.g., Rebay et al., 2010).

During the prograde *P-T* path of our samples, a significant portion of Sr and Pb may have first been hosted in lawsonite (as indicated by inclusions composed of paragonite + clinozoisite in garnet; e.g., Fig. 3A). Accompanied by prograde-retrograde *P-T* transition (see Fig. 4) and continued heating for a period thereafter with decreased *P/T* ratios, (clino)zoisite replaced lawsonite and scavenged the liberated Sr and Pb. The presence of prograde (clino)zoisite indicates that some of the Sr and Pb may also have been largely hosted in (clino)zoisite because of less H<sub>2</sub>O available in the original system (the H<sub>2</sub>O content determines the modal lawsonite under blueschist facies, i.e., the higher H<sub>2</sub>O content, the more lawsonite may form; e.g., Rebay et al., 2010; Poli and Schmidt, 1997). Up to about ~100 km, or even greater depths in relatively cold subduction zones (~12 GPa; Schmidt, 1995), although a portion of Pb and Sr could be transported further by K-hollandite and allanite, more (clino)zoisite or lawsonite will transform to garnet and omphacite, which cannot further accommodate Sr and Pb. Consequently, these two elements, or at least a large portion of them if not in their entirety, will be liberated along with released fluids into the subduction channel and, perhaps, contribute to the partial melting of the mantle wedge forearc (perhaps also backarc) magmatism (Fig. 12).

If paragonite were present prior to dehydration during subduction-zone metamorphism, LILEs would be transported within the subducted crust to a depth of at least ~70 km. If subducting sedimentary rocks and rocks of E-MORB-like or OIB-like protoliths with adequate K to produce muscovite are available at the early stage of metamorphism, then Rb, Ba,



**Figure 12.** Schematic diagram showing multistage subduction-zone metamorphism (SZM; modified from Poli and Schmidt, 2002). The stability of significant minerals in the subducted/subducting slab along the subduction zone is labeled, including allanite, the stability of which has been indicated following Hermann's experimental study (2002). The distinctive geochemical responses of key trace elements to the mineral stability are also shown, based on our samples, which have subducted to no less than 75 km. REE—rare earth element; HFSE—high field strength element; P/D—parent/daughter.

and Cs will be stabilized (refer to Figs. 11D2–E2 for the trace-element redistributed model) until the muscovite breakdown at a depth up to ~300 km (e.g., Sorensen et al., 1997; Poli and Schmidt, 2002). If no further minerals have already been produced (e.g., K-hollandite; Rapp et al., 2008) for hosting these elements or if the supercritical fluids or melts are present, these elements will contribute to the observed enrichment in backarc magmatism (Fig. 12). Otherwise, if no paragonite or phengitic muscovite was present before dehydration reactions during subduction-zone metamorphism, these elements will be released with fluids beneath the forearc (see Figs. 11D1–E1 for the expected trace-element redistribution), which is most likely the case for subducting depleted N-MORB-like rocks without significant seafloor alterations (i.e., low K and H<sub>2</sub>O).

Elements such as LREEs, U, and Th, which are typically enriched in volcanic arc basalts (e.g., Dilek and Furnes, 2011), have previously been considered as being mobile elements in subduction-zone metamorphism (e.g., McCulloch and Gamble, 1991). Our studies, however, have shown the immobility of these elements in rocks of both sedimentary and basaltic protoliths, i.e., the correlated variations among these elements were maintained prior to and during subduction-zone metamorphism. This indicates

that LREEs, U, and Th have not been released during subduction-zone metamorphism and would contribute little to subduction-zone magmatism as a function of dehydration, at least up to the peak conditions of these rocks (i.e., 75 km). Therefore, if the enrichments of these elements in arc lavas are indeed derived from the subducted ocean crust with the overlying sediments, other mechanisms, such as supercritical fluids or hydrous melts (which may happen at deeper depths), rather than simple metamorphic dehydration of aqueous fluids, are required. This is an important conclusion that encourages reconsideration of the standard model (“flux melting”) for arc magmatism.

#### Redox Conditions in Subduction Zones

Another important feature in the standard subduction model is its presumed highly oxidized state, as indicated by high Fe<sup>3+</sup>/Fe<sup>2+</sup> observed in arc volcanic rocks and in spinels from subarc mantle xenoliths. These oxidized conditions in the mantle wedge (unlike the more reduced condition in other tectonic settings, e.g., the asthenospheric mantle beneath mid-ocean ridges) are thought to be caused by the addition of slab-derived fluids (e.g., Wood et al., 1990; Brandon and Draper, 1996). However, based on V/Sc ratios in subarc peridotites and arc lavas rather than Fe<sup>3+</sup>/Fe<sup>2+</sup>, Lee et al. (2003,

2005) proposed that the oxygen fugacity in arc magma sources is actually similar to that of asthenospheric mantle beneath ocean ridges, i.e., as low as  $-1.25$ – $0.5$  log units relative to the FMQ (fayalite-magnetite-quartz) buffer. They also pointed out that it is inappropriate to use  $\text{Fe}^{3+}/\text{Fe}^{2+}$ , which only reflects the redox state in the last equilibrium process without any record of previous equilibrium history. The observation of  $\text{CH}_4$  fluid inclusions in olivine from a mantle wedge harzburgite sampled from the Qilian suture zone, northwest China (Song et al., 2009), also indicates that the actual redox state in subduction zones may be more reduced than widely assumed.

Since U becomes fluid soluble or mobile only as  $\text{U}^{6+}$  under oxidized conditions (e.g., Langmuir, 1978; Niu, 2004), the existence of a significant U-Th correlation (Fig. 8F; not only in our samples, but also in samples from other studies in the literature) and the absence of fractionations of U from Nb (Fig. 8E) indicate the immobility of U, which may be in response to the form of  $\text{U}^{4+}$  (vs.  $\text{U}^{6+}$ ) during subduction-zone metamorphism. These observations, together with the identification of graphite inclusions in porphyroblastic garnet from eclogite in western Tianshan (Lü et al., 2008, 2009), all indicate that subduction-zone metamorphism may indeed take place in a more reduced environment than previously thought. However, this is an open question, i.e., the immobility of U could also be controlled by other effects (e.g., stronger host mineral controls). More effort is needed to understand the oxidation state of subduction zones at UHP metamorphism conditions, which has the potential to improve understanding of subduction-zone magmatism.

### Implications for Mantle Compositional Heterogeneities

We have argued that fluids and a portion of fluid-soluble elements (i.e., LILEs, Sr, and Pb) could be released into the mantle wedge from rocks of basaltic protolith, while rocks of sedimentary protolith may host K, Rb, Cs, and Ba in phengite, stable up to depths of  $\sim 300$  km. At greater depths, K-hollandite could become the stable phase hosting these elements (Rapp et al., 2008).

Because our samples may not have been subducted beyond the depth more typical for subduction-zone magmatism (i.e.,  $\sim 100$  km according to Tatsumi and Kogiso, 2003), they may not represent the actual  $[\text{P}/\text{D}]_{\text{out}}$  brought to the deep mantle (see Figs. 1 and 12). However, systematic studies of the controls on the behavior of different elements and the direct geochemical consequence of subduction-zone metamorphism

as a function of dehydration for depths  $>75$  km in our study still allow us to reasonably infer the  $[\text{P}/\text{D}]_{\text{out}}$  into the deeper mantle. Therefore, we selected several eclogitic samples with minimal retrograde metamorphic overprints from group 1 and group 3 (the samples shown in bold in Table DR1 [see footnote 1]) and plotted their P/D ratios against ratios of immobile elements (i.e., Nb/Zr and Th/U) (Fig. 13). With relatively constant Nb/Zr and Th/U ratios in each group, Rb/Sr and U/Pb ratios vary significantly (Figs. 13A–13D), which is expected because Rb, Sr, and Pb are mobile. In contrast, Sm/Nd and Lu/Hf ratios are almost constant (Figs. 13E–13H), consistent with their inherited magmatic signature and immobile behavior during subduction-zone metamorphism. These observations indicate that

the element mobility/immobility may not only alter the element content, but it could also affect element ratios.

As radiogenic isotope ratios are a function of time, they may reflect the time-integrated evolution of radioactive parent to radiogenic daughter (P/D) in the ultimate subducted materials in the mantle. Together with several selected eclogitic metabasites from other locations in the world (Table DR6 [see footnote 1]), Sm/Nd consistently shows good correlation with Lu/Hf (Fig. 14B) but lacks correlation with Rb/Sr (Fig. 14A). When these rocks return into mantle source regions for oceanic basalts, they cannot contribute to the first-order negative Sr-Nd isotope correlation observed in oceanic basalts (Fig. 14A, inset; also see fig. 4a in Niu and

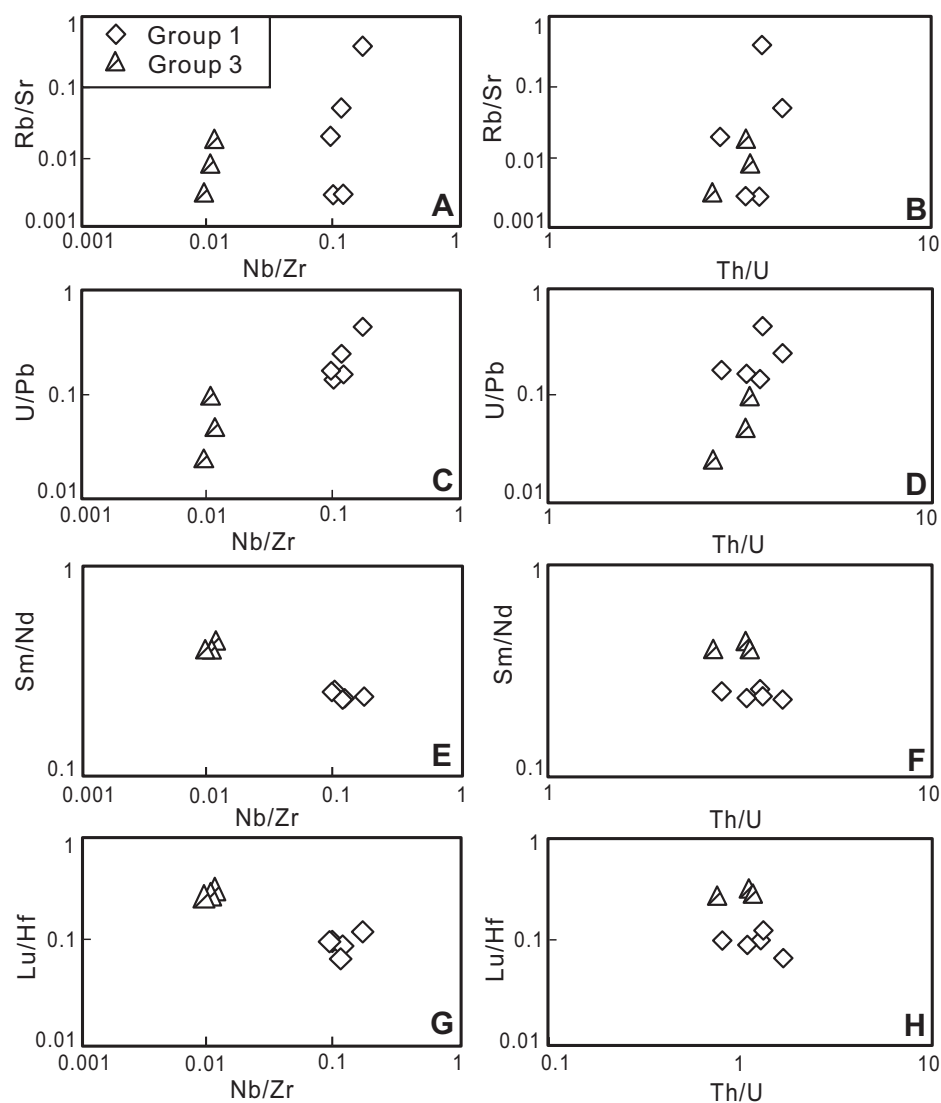
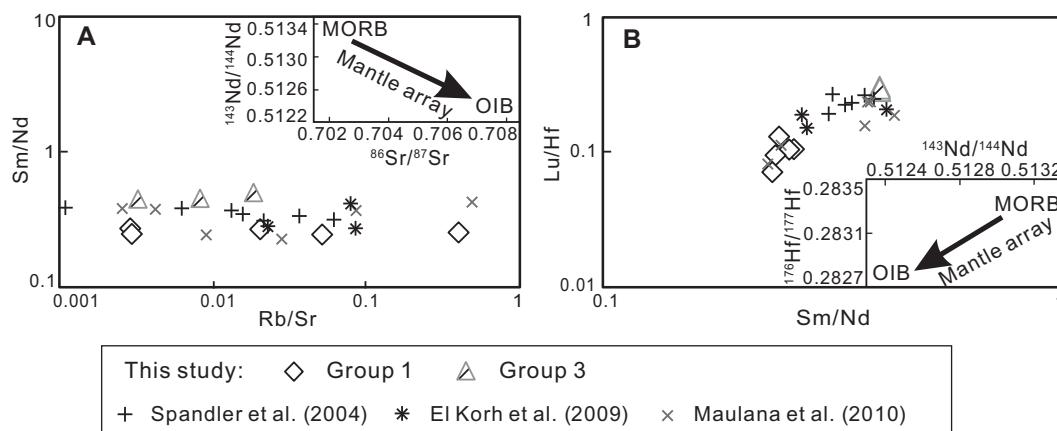


**Figure 13.** Scatter plots of parent/daughter (P/D) ratios (i.e., Rb/Sr, U/Pb, Sm/Nd, and Lu/Hf) against immobile element ratios (Nb/Zr and Th/U) for samples with minimal retrograde overprints (samples labeled in bold in Table DR1 [see text footnote 1]).

**Figure 14. Comparisons of parent/daughter (P/D) ratios with radiogenic isotope ratios (the two insets are adapted from Hofmann [1997] and White and Patchett [1984]). Selected samples are the same as those in Figure 13. Several selected eclogitic metabasites in the literature are also plotted, and the relevant values are given in Table DR6 (see text footnote 1). The positive Sm/Nd-Lu/Hf correlation is consistent with these rocks being potential source materials for ocean-island basalts (OIBs) when subducted with a positive Hf-Nd isotopic relationship, but the lack of Rb/Sr-Sm/Nd (and Lu/Hf) correlation is inconsistent with the rocks being the major source materials for oceanic basalts that show significant inverse Sr-Nd and Sr-Hf isotopic systematics. MORB—mid-ocean-ridge basalt.**



O'Hara, 2003), even though the significant positive Sm/Nd-Lu/Hf correlation is apparently consistent with the  $^{143}\text{Nd}/^{144}\text{Nd}$  versus  $^{176}\text{Hf}/^{177}\text{Hf}$  correlation in oceanic basalts (Fig. 14B, inset; also see fig. 4b in Niu and O'Hara, 2003). Therefore, the subducted ocean crust cannot be the major source materials of oceanic basalts in terms of Sr-Nd-Pb radiogenic isotopes (also see Niu and O'Hara, 2003; Niu, 2004).

The immobility of U during subduction-zone metamorphism and Pb fractionation in the subducting/subducted crust indicate that U/Pb in the subducted crust will have increased  $[\text{P/D}]_{\text{out}}$  and will lead to a higher ratio of U/Pb in the deep mantle (there may be an elevated ratio of Th/Pb as well because of the similar behavior of Th and U during subduction-zone metamorphism; e.g., Fig. 8F). Therefore, such fractionations of U-Th (especially U) from Pb may contribute to the source of HIMU.

## CONCLUSIONS

We have attempted to characterize elemental behaviors in response to subduction-zone metamorphism using detailed petrography and bulk-rock geochemistry of subduction-zone UHP metamorphic rocks from Chinese western Tianshan. Several tentative conclusions are:

(1) Based on the studies of immobile elements, our samples of basaltic protolith can be divided into three groups: Group 1 points to a protolith resembling the present-day average OIB (or enriched seamount lavas); the protoliths of group 2 are similar to N-MORB melts contaminated by a continental crustal component; and the protoliths of group 3 are akin to highly depleted MORB. The association of these diverse metabasaltic compositions together with

rocks of sedimentary protolith indicates that the input into subduction zones can be diverse, and may represent a tectonic mélange composed of normal ocean crust with dismembered seamounts, sediments, and arc-derived materials. We have also argued that the composition of the protolith plays an important role in determining the mineral assemblages and elemental fractionations during subduction-zone metamorphism.

(2) We have demonstrated and confirmed that HFSEs and REEs are in general immobile during subduction-zone metamorphism. The significant correlation of U with Th (and Nb) indicates that U is immobile and may point to a reduced environment, contrary to the common perception that subduction zones are relatively oxidized. The immobility of LREEs, U, and Th further implies that, at least in the absence of supercritical fluids or hydrous melts, these elements may not contribute to subduction-zone magmatism under metamorphic conditions of our study, i.e., up to ~80 km depth (i.e., >~2.5 GPa). In addition, the immobility of U in this study suggests that the component of altered ocean crust, if involved at all, is insignificant in the protoliths of our samples.

(3) LILEs including Sr and Pb in rocks of basaltic protolith have been mobilized, although it is not clear whether this happened at the same time for all samples. LILEs in metasedimentary rocks appear to have remained immobile, most likely because these elements are largely hosted in white mica, which is stable over much of the subduction-zone metamorphism conditions. For metabasaltic rocks, the timing of the appearance and stability of white mica during seafloor subduction is important in determining the mobility/immobility of their preferentially hosted elements. However, further studies on

trace-element budgets in natural samples from other HP and UHP metamorphic suites are needed to verify this result.

(4) Compared with the abundances and ratios of immobile elements, we confirm that both abundances and ratios of mobile elements have been altered during subduction-zone metamorphism, and hence the  $[\text{P/D}]_{\text{in}}$  (i.e., Rb/Sr and U/Pb input into the trench) differs from the  $[\text{P/D}]_{\text{out}}$  of subduction-zone metamorphic systems. Therefore, it is inappropriate and misleading to use  $[\text{P/D}]_{\text{out}}$  in the subducting crust, inferred from oceanic basalts, to constrain the  $[\text{P/D}]_{\text{in}}$  of surface rocks that have entered trenches.

## ACKNOWLEDGMENTS

The sampling was conducted in 2002 and supported by a Natural Environment Research Council (NERC) Senior Research Fellowship to Yaoling Niu, a NERC studentship to Shaun Lavis, and a Royal Society China joint project, Chinese National Science Foundation (NSF), and Chinese Geological Survey. The analytical work was done by Shaun Lavis as a part of his Ph.D. research work, supported by Higher Education Funding Council for England (HEFCE)/NERC grants to Julian A. Pearce and Yaoling Niu and other NERC grants to Julian A. Pearce. Yaoling Niu also thanks Leverhulme Trust for a research fellowship, Durham University for a Christopherson/Knott Fellowship, and Chinese NSF for partial supports (grants 9101400, 41130314). Yuanyuan Xiao was supported by a Durham University doctoral fellowship. Comments from the associate editors (William Peck and Yildirim Dilek) and reviewers (Timm John, Lifei Zhang, Ali Polat, and two anonymous reviewers) are gratefully appreciated and have helped to improve this paper.

## REFERENCES CITED

Ai, Y.L., Zhang, L.F., Li, X.P., and Qu, J.F., 2006, Geochemical characteristics and tectonic implications of HP-UHP eclogites and blueschists in southwestern Tianshan, China: Progress in Natural Science, v. 16, no. 6, p. 624–632, doi:10.1080/10020070612330044.

- Ando, A., Mita, N., and Terashima, S., 1987, 1986 values for fifteen GSJ rock reference samples: Igneous rock series: *Geostandards Newsletter*, v. 11, p. 159–166, doi:10.1111/j.1751-908X.1987.tb00023.x.
- Bebout, G.E., 2007, Metamorphic chemical geodynamics of subduction zones: *Earth and Planetary Science Letters*, v. 260, p. 373–393, doi:10.1016/j.epsl.2007.05.050.
- Becker, H., Jochum, K.P., and Carlson, R.W., 2000, Trace element fractionation during dehydration of eclogites from high-pressure terranes and the implications for element fluxes in subduction zones: *Chemical Geology*, v. 163, p. 65–99, doi:10.1016/S0009-2541(99)00071-6.
- Beinlich, A., Klemd, R., John, T., and Gao, J., 2010, Trace-element mobilization during Ca-metasomatism along a major fluid conduit: Eclogitization of blueschist as a consequence of fluid-rock interaction: *Geochimica et Cosmochimica Acta*, v. 74, p. 1892–1922, doi:10.1016/j.gca.2009.12.011.
- Brandon, A.D., and Draper, D.S., 1996, Constraints on the origin of the oxidation state of mantle overlying subduction zones—An example from Simcoe, Washington, USA: *Geochimica et Cosmochimica Acta*, v. 60, p. 1739–1749, doi:10.1016/0016-7037(96)00056-7.
- Cann, J.R., 1970, Rb, Sr, Y, Zr and Nb in some ocean floor basaltic rocks: *Earth and Planetary Science Letters*, v. 10, p. 7–11, doi:10.1016/0012-821X(70)90058-0.
- Dilek, Y., and Furnes, H., 2011, Ophiolite genesis and global tectonics: Geochemical and tectonic fingerprinting of ancient oceanic lithosphere: *Geological Society of America Bulletin*, v. 123, p. 387–411, doi:10.1130/B30446.1.
- Donnelly, K.E., Goldstein, S.L., Langmuir, C.H., and Spiegelman, M., 2004, Origin of enriched ocean ridge basalts and implications for mantle dynamics: *Earth and Planetary Science Letters*, v. 226, p. 347–366, doi:10.1016/j.epsl.2004.07.019.
- El Korh, A., Schmidt, S.T., Ulianov, A., and Potel, S., 2009, Trace element partitioning in HP-LT metamorphic assemblages during subduction-related metamorphism, Ile de Groix, France: A detailed LA-ICPMS study: *Journal of Petrology*, v. 50, p. 1107–1148, doi:10.1093/petrology/egg034.
- Feineman, M.D., Ryerson, F.J., DePaolo, D.J., and Plank, T., 2007, Zoisite-aqueous fluid trace element partitioning with implications for subduction zone fluid composition: *Chemical Geology*, v. 239, p. 250–265, doi:10.1016/j.chemgeo.2007.01.008.
- Gao, J., and Klemd, R., 2003, Formation of HP-LT rocks and their tectonic implications in the western Tianshan orogen, NW China: *Geochemical and age constraints: Lithos*, v. 66, p. 1–22, doi:10.1016/S0024-4937(02)00153-6.
- Gao, J., Long, L.L., Qian, Q., Huang, D.Z., Su, W., and Klemd, R., 2006, South Tianshan: A late Paleozoic or a Triassic orogen?: *Acta Petrologica Sinica*, v. 22, no. 5, p. 1049–1061.
- Gao, J., John, T., Klemd, R., and Xiong, X.M., 2007, Mobilization of Ti-Nb-Ta during subduction: Evidence from rutile-bearing dehydration segregations and veins hosted in eclogite, Tianshan, NW China: *Geochimica et Cosmochimica Acta*, v. 71, p. 4974–4996, doi:10.1016/j.gca.2007.07.027.
- Gao, J., Long, L.L., Klemd, R., Qian, Q., Liu, D.Y., Xiong, X.M., Su, W., Liu, W., Wang, Y.T., and Yang, F.Q., 2009, Tectonic evolution of the South Tianshan orogen and adjacent regions, NW China: *Geochemical and age constraints of granitoid rocks: International Journal of Earth Sciences*, v. 98, p. 1221–1238, doi:10.1007/s00531-008-0370-8.
- Hermann, J., 2002, Allanite: Thorium and light rare earth element carrier in subducted crust: *Chemical Geology*, v. 192, p. 289–306, doi:10.1016/S0009-2541(02)00222-X.
- Hermann, J., Spandler, C., Hack, A., and Korsakov, A.V., 2006, Aqueous fluids and hydrous melts in high-pressure and ultra-high pressure rocks: Implications for element transfer in subduction zones: *Lithos*, v. 92, p. 399–417, doi:10.1016/j.lithos.2006.03.055.
- Hofmann, A.W., 1997, Mantle geochemistry: The message from oceanic volcanism: *Nature*, v. 385, p. 219–229, doi:10.1038/385219a0.
- Hofmann, A.W., and Hart, S.R., 1978, An assessment of local and regional isotopic equilibrium in the mantle: *Earth and Planetary Science Letters*, v. 38, p. 44–62, doi:10.1016/0012-821X(78)90125-5.
- Hofmann, A.W., Jochum, K.P., Seufert, M., and White, W.M., 1986, Nb and Pb in oceanic basalts: New constraints on mantle evolution: *Earth and Planetary Science Letters*, v. 79, p. 33–45, doi:10.1016/0012-821X(86)90038-5.
- John, T., Scherer, E.E., Haase, K., and Schenk, V., 2004, Trace element fractionation during fluid-induced eclogitization in a subducting slab: Trace element and Lu-Hf-Sm-Nd isotope systematic: *Earth and Planetary Science Letters*, v. 227, p. 441–456, doi:10.1016/j.epsl.2004.09.009.
- John, T., Klemd, R., Gao, J., and Garbe-Schönberg, C.D., 2008, Trace-element mobilization in slabs due to non steady-state fluid-rock interaction: Constraints from an eclogite-facies transport vein in blueschist (Tianshan, China): *Lithos*, v. 103, p. 1–24, doi:10.1016/j.lithos.2007.09.005.
- Kelley, K.A., Plank, T., Ludden, J., and Staudigel, H., 2003, Composition of altered oceanic crust at ODP Sites 801 and 1149: *Geochemistry, Geophysics, Geosystems*, v. 4, doi:10.1029/2002GC000435.
- Kelley, K.A., Plank, T., Farr, L., Ludden, J., and Staudigel, H., 2005, Subduction cycling of U, Th and Pb: *Earth and Planetary Science Letters*, v. 234, p. 369–383, doi:10.1016/j.epsl.2005.03.005.
- Kessel, R., Schmidt, M.W., Ulmer, P., and Pettke, T., 2005, Trace element signature of subduction—Zone fluids, melts and supercritical liquids at 120–180 km depth: *Nature*, v. 437, p. 724–727, doi:10.1038/nature03971.
- Klemd, R., 2003, Ultrahigh-pressure metamorphism in eclogites from the western Tianshan high-pressure belt (Xinjiang, western China)—Comment: *The American Mineralogist*, v. 88, p. 1153–1156.
- Langmuir, D., 1978, Uranium solution-mineral equilibria at low temperatures with applications to sedimentary ore deposits: *Geochimica et Cosmochimica Acta*, v. 42, p. 547–569, doi:10.1016/0016-7037(78)90001-7.
- Lavis, S., 2005, Recycling in Subduction Zones: Evidence from Eclogites and Blueschist of NW China [Ph.D. thesis]: Cardiff, UK, Cardiff University, 245 p.
- Leake, B.E., Woolley, A.R., Arps, C.E.S., Birch, W.D., Gilbert, M.C., Grice, J.D., Hawthorne, F.C., Kato, A., Kisch, H.J., Krivovichev, V.G., Linthout, K., Laird, J., Mandarino, J.A., Maresch, W.V., Nickel, E.H., Rock, N.M.S., Schumacher, J.C., Smith, D.C., Stephenson, N.C.N., Ungaretti, L., Whittaker, E.J.W., and Youshi, G., 1997, Nomenclature of amphiboles: Report of the Subcommittee on Amphiboles of the International Mineralogical Association, Commission on New Minerals and Mineral Names: *Canadian Mineralogist*, v. 35, p. 219–246.
- Lee, C.-T.A., Brandon, A.D., and Norman, M., 2003, Vanadium in peridotites as a proxy for paleo- $fO_2$  during partial melting: Prospects, limitations, and implications: *Geochimica et Cosmochimica Acta*, v. 67, p. 3045–3064, doi:10.1016/S0016-7037(03)00268-0.
- Lee, C.-T.A., Leeman, W.P., Canil, D., and Li, Z.-X.A., 2005, Similar V/Sc systematics in MORB and arc basalts: Implications for the oxygen fugacities of their mantle source regions: *Journal of Petrology*, v. 46, p. 2313–2336, doi:10.1093/petrology/egi056.
- Liu, J., Bohlen, S.R., and Ernst, W.G., 1996, Stability of hydrous phases in subducting oceanic crust: *Earth and Planetary Science Letters*, v. 143, p. 161–171, doi:10.1016/0012-821X(96)00130-6.
- Lü, Z., Zhang, L.F., Du, J.X., and Bucher, K., 2008, Coesite inclusions in garnet from eclogitic rocks in western Tianshan, northwest China: Convincing proof of UHP metamorphism: *The American Mineralogist*, v. 93, p. 1845–1850, doi:10.2138/am.2008.2800.
- Lü, Z., Zhang, L.F., Du, J.X., and Bucher, K., 2009, Petrology of coesite-bearing eclogite from Habutengsu Valley, western Tianshan, NW China, and its tectono-metamorphic implication: *Journal of Metamorphic Geology*, v. 27, p. 773–787, doi:10.1111/j.1525-1314.2009.00845.x.
- Manning, C.E., 2004, The chemistry of subduction-zone fluids: *Earth and Planetary Science Letters*, v. 223, p. 1–16, doi:10.1016/j.epsl.2004.04.030.
- Maulana, A., Ellis, D.J., and Christy, A.G., 2010, Petrology, geochemistry and tectonic evolution of the south Sulawesi basement rocks, Indonesia, in *Proceedings of the Indonesian Petroleum Association: Indonesian Petroleum Association, IPA10-G-192*.
- McCulloch, M.T., and Gamble, J.A., 1991, Geochemical and geodynamical constraints on subduction zone magmatism: *Earth and Planetary Science Letters*, v. 102, p. 358–384, doi:10.1016/0012-821X(91)90029-H.
- Morimoto, N., 1988, Nomenclature of pyroxenes: *Mineralogy and Petrology*, v. 39, p. 55–76, doi:10.1007/BF01226262.
- Niu, Y.L., 2004, Bulk-rock major and trace element compositions of abyssal peridotites: Implications for mantle melting, melt extraction and post-melting processes beneath mid-ocean ridges: *Journal of Petrology*, v. 45, p. 2423–2458, doi:10.1093/petrology/egh068.
- Niu, Y.L., 2009, Some basic concepts and problems on the petrogenesis of intra-plate ocean island basalts: *Chinese Science Bulletin*, v. 54, p. 4148–4160, doi:10.1007/s11434-009-0668-3.
- Niu, Y.L., and Batiza, R., 1997, Trace element evidence from seamounts for recycled oceanic crust in the eastern equatorial Pacific mantle: *Earth and Planetary Science Letters*, v. 148, p. 471–484, doi:10.1016/S0012-821X(97)00048-4.
- Niu, Y.L., and O'Hara, M.J., 2003, Origin of ocean island basalts: A new perspective from petrology, geochemistry, and mineral physics considerations: *Journal of Geophysical Research*, v. 108, p. ECV5.1–ECV5.19, doi:10.1029/2002JB002048.
- O'Nions, R.K., Evensen, N.M., and Hamilton, P.J., 1979, Geochemical modelling of mantle differentiation and crustal growth: *Journal of Geophysical Research*, v. 84, p. 6091–6101, doi:10.1029/JB084iB11p06091.
- Page, F.Z., Essene, E.J., and Mukasa, S.B., 2005, Quartz exsolution in clinopyroxene is not proof of ultrahigh pressures: Evidence from eclogites from the Eastern Blue Ridge, Southern Appalachians, U.S.A.: *The American Mineralogist*, v. 90, p. 1092–1099, doi:10.2138/am.2005.1761.
- Pawley, A.R., and Holloway, J.R., 1993, Water sources for subduction zone volcanism: New experimental constraints: *Science*, v. 260, p. 664–667, doi:10.1126/science.260.5108.664.
- Peacock, S.M., 1993, The importance of blueschist-eclogite dehydration reactions in subducting oceanic crust: *Geological Society of America Bulletin*, v. 105, p. 684–694, doi:10.1130/0016-7606(1993)105<0684:TIOBED>2.3.CO;2.
- Pearce, J.A., 1996, A user's guide to basalt discrimination diagrams, in Wyman, D.A., ed., *Trace Element Geochemistry of Volcanic Rocks: Implications for Massive Sulphide Exploration: Geological Association of Canada Special Publication 12*, p. 79–113.
- Pearce, J.A., 2008, Geochemical fingerprinting of oceanic basalts with applications to ophiolite classification and the search for Archean oceanic crust: *Lithos*, v. 100, p. 14–48, doi:10.1016/j.lithos.2007.06.016.
- Pearce, J.A., and Cann, J.R., 1973, Tectonic setting of basic volcanic rocks determined using trace element analyses: *Earth and Planetary Science Letters*, v. 19, p. 290–300, doi:10.1016/0012-821X(73)90129-5.
- Pilchin, A., 2005, The role of serpentinization in exhumation of high- to ultra-high-pressure metamorphic rocks: *Earth and Planetary Science Letters*, v. 237, p. 815–828, doi:10.1016/j.epsl.2005.06.053.
- Pilet, S., Baker, M.B., and Stolper, E.M., 2008, Metasomatized lithosphere and the origin of alkaline lavas: *Science*, v. 320, p. 916–919, doi:10.1126/science.1156563.
- Plank, T., and Langmuir, C.H., 1998, The chemical composition of subducting sediment and its consequences for the crust and mantle: *Chemical Geology*, v. 145, p. 325–394, doi:10.1016/S0009-2541(97)00150-2.
- Poli, S., and Schmidt, M.W., 1997, The high-pressure stability of hydrous phases in orogenic belts: An experimental approach on eclogite-forming processes: *Tectonophysics*, v. 273, p. 169–184, doi:10.1016/S0040-1951(96)00293-4.
- Poli, S., and Schmidt, M.W., 1998, The high-pressure stability of zoisite and phase relationships of zoisite-bearing assemblages: Contributions to Mineralogy and Petrology, v. 130, p. 162–175, doi:10.1007/s004100050357.

- Poli, S., and Schmidt, M.W., 2002, Petrology of subducted slabs: Annual Review of Earth and Planetary Sciences, v. 30, p. 207–235, doi:10.1146/annurev.earth.30.091201.140550.
- Rapp, R.P., Irifune, T., Shimizu, N., Nishiyama, N., Norman, M.D., and Inoue, T., 2008, Subduction recycling of continental sediments and the origin of geochemically enriched reservoirs in the deep mantle: Earth and Planetary Science Letters, v. 271, p. 14–23, doi:10.1016/j.epsl.2008.02.028.
- Rebay, G., Powell, R., and Diener, J.F.A., 2010, Calculated phase equilibria for a MORB composition in a *P-T* range, 450–650 °C and 18–28 kbar: The stability of eclogite: Journal of Metamorphic Geology, v. 28, p. 635–645, doi:10.1111/j.1525-1314.2010.00882.x.
- Reinecke, T., 1998, Prograde high- to ultrahigh-pressure metamorphism and exhumation of oceanic sediments at Lago di Cignana, Zermatt-Saas zone, western Alps: Lithos, v. 42, p. 147–189, doi:10.1016/S0024-4937(97)00041-8.
- Schmidt, M.W., 1995, Lawsonite: Upper pressure stability and formation of higher density hydrous phases: The American Mineralogist, v. 80, p. 1286–1292.
- Schmidt, M.W., and Poli, S., 1998, Experimentally based water budgets for dehydrating slabs and consequences for arc magma generation: Earth and Planetary Science Letters, v. 163, p. 361–379, doi:10.1016/S0012-821X(98)00142-3.
- Schmidt, M.W., and Poli, S., 2003, Generation of mobile components during subduction of oceanic crust, in Rudnick, R.L., ed., The Crust: Treatise on Geochemistry, Volume 3: New York, Elsevier, p. 567–591.
- Smit, M.A., Bröcker, M., and Scherer, E.E., 2008, Aragonite and magnesite in eclogites from the Jæren nappe, SW Norway: Disequilibrium in the system CaCO<sub>3</sub>–MgCO<sub>3</sub> and petrological implications: Journal of Metamorphic Geology, v. 26, p. 959–979, doi:10.1111/j.1525-1314.2008.00795.x.
- Song, S.G., Su, L., Niu, Y.L., Lai, Y., and Zhang, L.F., 2009, CH<sub>4</sub> inclusions in orogenic harzburgite: Evidence for reduced slab fluids and implication for redox melting in mantle wedge: Geochimica et Cosmochimica Acta, v. 73, p. 1737–1754, doi:10.1016/j.gca.2008.12.008.
- Sorensen, S.S., Grossman, J.N., and Perfit, M.R., 1997, Phengite-hosted LILE enrichment in eclogite and related rocks: Implications for fluid-mediated mass transfer in subduction zones and arc magma genesis: Journal of Petrology, v. 38, p. 3–34, doi:10.1093/petrology/38.1.3.
- Spandler, C., Hermann, J., Arculus, R., and Mavrogenes, J., 2003, Redistribution of trace elements during prograde metamorphism from lawsonite blueschist to eclogite facies: Implications for deep subduction-zone processes: Contributions to Mineralogy and Petrology, v. 146, p. 205–222, doi:10.1007/s00410-003-0495-5.
- Spandler, C., Hermann, J., Arculus, R., and Mavrogenes, J., 2004, Geochemical heterogeneity and element mobility in deeply subducted oceanic crust: insights from high-pressure mafic rocks from New Caledonia: Chemical Geology, v. 206, p. 21–42, doi:10.1016/j.chemgeo.2004.01.006.
- Su, W., Gao, J., Klemm, R., Li, J.L., Zhang, X., Li, X.H., Chen, N.S., and Zhang, L., 2010, U-Pb zircon geochronology of Tianshan eclogites in NW China: Implication for the collision between the Yili and Tarim blocks of the southwestern Altai: European Journal of Mineralogy, v. 22, p. 473–478, doi:10.1127/0935-1221/2010/0022-2040.
- Sun, S.S., and McDonough, W.F., 1989, Chemical and isotopic systematics in ocean basalt: Implication for mantle composition and processes, in Saunders, A.D., and Norry, M.J., eds., Magmatism in the Ocean Basins: Geological Society of London Special Publication 42, p. 313–345, doi:10.1144/GSL.SP.1989.042.01.19.
- Tatsumi, Y., and Kogiso, T., 2003, The subduction factory: Its role in the evolution of the Earth's crust and mantle, in Larter, R.D., and Leat, P.T., eds., Intra-Oceanic Subduction Systems: Tectonic and Magmatic Processes: Geological Society of London Special Publication 219, p. 55–80.
- van der Straaten, F., Schenk, V., John, T., and Gao, J., 2008, Blueschist-facies rehydration of eclogites (Tian Shan, NW-China): Implications for fluid-rock interaction in the subduction channel: Chemical Geology, v. 255, p. 195–219, doi:10.1016/j.chemgeo.2008.06.037.
- Volkova, N.I., and Budanov, V.I., 1999, Geochemical discrimination of metabasalt rocks of the Fan-Karatagin transitional blueschist/greenschist belt, South Tianshan, Tajikistan: Seamount volcanism and accretionary tectonics: Lithos, v. 47, p. 201–216, doi:10.1016/S0024-4937(99)00019-5.
- Weaver, B.L., 1991, The origin of ocean island end-member compositions: Trace element and isotopic constraints: Earth and Planetary Science Letters, v. 104, p. 381–397, doi:10.1016/0012-821X(91)90217-6.
- White, W.M., 1985, Sources of oceanic basalts: Radiogenic isotopic evidence: Geology, v. 13, p. 115–118.
- White, W.M., and Patchett, J., 1984, Hf-Nd-Sr isotopes and incompatible element abundances in island arcs: Implications for magma origins and crust-mantle evolution: Earth and Planetary Science Letters, v. 67, p. 167–185, doi:10.1016/0012-821X(84)90112-2.
- Willbold, M., and Stracke, A., 2006, Trace element composition of mantle end-members: Implications for recycling of oceanic and upper and lower continental crust: Geochemistry, Geophysics, Geosystems, v. 7, doi:10.1029/2005GC001005.
- Winchester, J.A., and Floyd, P.A., 1977, Geochemical discrimination of different magma series and their differentiation products using immobile elements: Chemical Geology, v. 20, p. 325–343, doi:10.1016/0009-2541(77)90057-2.
- Wood, B.J., Bryndzia, L.T., and Johnson, K.E., 1990, Mantle oxidation state and its relationship to tectonic environment and fluid speciation: Science, v. 248, p. 337–345, doi:10.1126/science.248.4953.337.
- Yu, Z.S., Robinson, P., and McGoldrick, P., 2001, An evaluation of methods for the chemical decomposition of geological materials for trace element determination using ICP-MS: Geostandards Newsletter, v. 25, p. 199–217, doi:10.1111/j.1751-908X.2001.tb00596.x.
- Zack, T., and John, T., 2007, An evaluation of reactive fluid flow and trace element mobility in subducting slabs: Chemical Geology, v. 239, p. 199–216, doi:10.1016/j.chemgeo.2006.10.020.
- Zack, T., Rivers, T., and Foley, S.F., 2001, Cs-Rb-Ba systematics in phengite and amphibole: An assessment of fluid mobility at 2.0 GPa in eclogites from Trescolmen, Central Alps: Contributions to Mineralogy and Petrology, v. 140, p. 651–669, doi:10.1007/s004100000206.
- Zhang, L.F., Gao, J., Ekebair, S., and Wang, Z.X., 2001, Low temperature eclogite facies metamorphism in western Tianshan, Xinjiang: Science in China, v. 44, p. 85–96, doi:10.1007/BF02906888.
- Zhang, L.F., Ellis, D.J., and Jiang, W.B., 2002a, Ultrahigh-pressure metamorphism in western Tianshan, China: Part I. Evidence from inclusions of coesite pseudomorphs in garnet and from quartz exsolution lamellae in omphacite in eclogites: The American Mineralogist, v. 87, p. 853–860.
- Zhang, L.F., Ellis, D.J., Williams, S., and Jiang, W.B., 2002b, Ultra-high pressure metamorphism in western Tianshan, China: Part II. Evidence from magnesite in eclogite: The American Mineralogist, v. 87, p. 861–866.
- Zhang, L.F., Ellis, D.J., Arculus, R.J., Jiang, W., and Wei, C., 2003, 'Forbidden zone' subduction of sediments to 150 km depth—The reaction of dolomite + magnesite + aragonite in the UHP metamorphism metapelites from western Tianshan, China: Journal of Metamorphic Geology, v. 21, p. 523–529, doi:10.1046/j.1525-1314.2003.00460.x.
- Zhang, L.F., Song, S.G., Liou, J.G., Ai, Y.L., and Li, X.P., 2005, Relict coesite exsolution in omphacite from western Tianshan eclogites, China: The American Mineralogist, v. 90, p. 181–186, doi:10.2138/am.2005.1587.
- Zhang, L.F., Ai, Y.L., Li, X.P., Rubatto, D., Song, B., Williams, S., Song, S.G., Ellis, D., and Liou, J.G., 2007, Triassic collision of western Tianshan orogenic belt, China: Evidence from SHRIMP U-Pb dating of zircon from HP/UHP eclogitic rocks: Lithos, v. 96, p. 266–280, doi:10.1016/j.lithos.2006.09.012.
- Zindler, A., and Hart, S., 1986, Chemical geodynamics: Annual Review of Earth and Planetary Sciences, v. 14, p. 493–571, doi:10.1146/annurev.earth.14.050186.002425.

SCIENCE EDITOR: A. HOPE JAHREN

ASSOCIATE EDITOR: YILDIRIM DILEK

MANUSCRIPT RECEIVED 28 MARCH 2011

REVISED MANUSCRIPT RECEIVED 29 SEPTEMBER 2011

MANUSCRIPT ACCEPTED 9 DECEMBER 2011

Printed in the USA